1

The Classification of Galaxies

Ronald BUTA
Astrophysics, University of Alabama, Tuscaloosa, USA

The classification of the forms of galaxies in a well-defined visual system is a critical step in the study of galaxies as physical objects. The Comprehensive de Vaucouleurs revised Hubble-Sandage (CVRHS) system is currently the most detailed approach that can be applied effectively to more than 95% of all galaxies. This chapter describes the different types of galaxies and the factors that may determine various morphological features.

1.1. Introduction

Galaxies are complex gravitational systems whose structure has been influenced not only by how they formed but also by the environment into which they were born. A century ago, getting a classifiable image of a single galaxy was a major effort involving long exposures of photograph plates. Today, there are classifiable images of literally millions of galaxies available through the Internet. Although it is not obvious how any galaxy arrived at its current morphological state, examination of the details of large numbers of galaxies have led to important physical insights into the roles played by both internal and external processes. It is for this reason that classical galaxy morphology and classification have survived into the modern era.

Galaxy morphology and classification began with simple descriptive terms for angular size, brightness and central concentration based on visual observations (e.g. Dreyer 1888). Although large 19th-Century reflectors did reveal through visual observation some genuine aspects of galaxy morphology, it was photography that led

Galaxies,
coordinated by Françoise COMBES.

to the classification systems of the early-to-mid 20th Century, including those of Wolf (1908), Reynolds (1920), Hubble (1926, 1936), Lundmark (1926) and Morgan (1958). On the plates of the time, which were relatively more sensitive to blue light than to red light, details of spiral arms, disks and bulges could be used as classification criteria. In spite of great observational and theoretical progress in extragalactic studies during the past century, modern galaxy classification is still basically tied to the system proposed by Hubble (1936; Figure 1.1), only now the system is applied using digital images rather than photographic plates. The main reason the Hubble system has survived for nearly a century is that the aspects Hubble focused on (degree of central concentration, pitch angle and resolution of spiral arms, amount of distinct structure) correlated with measured properties of galaxies, such as luminosities, colors, stellar populations, HI content and global star formation history. This gave his view an astrophysically relevant edge that has driven much of extragalactic research since his time.

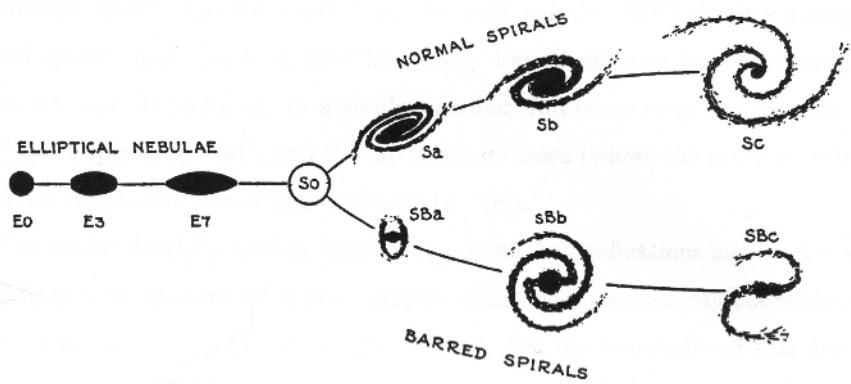

Figure 1.1. *The Hubble (1936) "tuning fork" representation of galaxy morphology*

This chapter describes the different classes of galaxies within the framework of the "Comprehensive de Vaucouleurs revised Hubble–Sandage" (CVRHS) classification system, a visual system that follows the precepts of de Vaucouleurs (1959), who proposed a personal revision of the Hubble–Sandage (HS) classification (Sandage 1961; Figure 1.2) that he believed provided a better description of galaxies without being too unwieldy. For many galaxies, the CVRHS classification is no more complicated than a de Vaucouleurs (1959) VRHS classification. However, the system has been designed to take into account more details that are of astrophysical interest today and which have become more noticeable and relevant in the era of digital astronomical imaging. These details include lenses, nuclear rings and bars, ansae

bars, boxy/peanut bulges, boxy and disky elliptical galaxies, special outer rings and pseudorings, dust lanes and galactic disk warps.

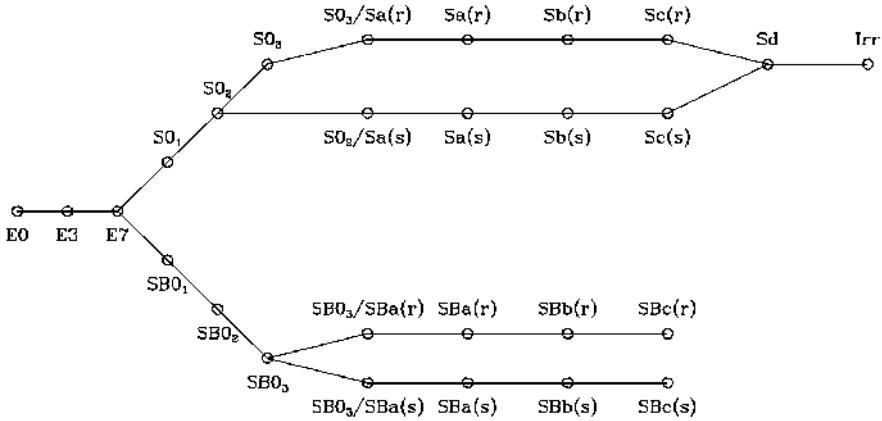

Figure 1.2. *The Hubble–Sandage (Sandage 1961) revised "tuning fork" representation of galaxy morphology, including stages of S0 galaxies*

1.2. Classes of galaxies

Hubble recognized that there are basically two classes of galaxies: disk-shaped galaxies and non-disk-shaped galaxies. In a disk galaxy, the structure is dominated by a highly flattened stellar component. Within this disk, other structures may be seen, such as spiral arms, bars, rings, a central bulge and extensive distributions of interstellar gas and dust. The way these structures are seen depends on the inclination of the plane of the disk to our line of sight. For a given galaxy, we say the inclination i is 0° when the disk is seen face-on, and 90° when the disk is seen edge-on. Disk planes are randomly oriented to the line of sight (meaning they are uniformly distributed in $\sin i$), which complicates the interpretation of highly inclined cases. Even a century ago, disk-shaped galaxies were known to be more common than non-disk galaxies to the point that the latter were considered of greater interest (Keeler 1899).

Although not all disk-shaped galaxies are spiral, the typical disk galaxy is a spiral, where luminous, outwardly winding arcs of stars and often star-forming regions form a major part of the morphology. Classic nearby spirals such as M51, M81, and M101 initially fueled the misperception that spirals are generally regular systems having only a bulge in addition to the disk and spiral arms. It was thought by Hubble that barred spirals are significantly less abundant than non-barred spirals, or what he called

"normal spirals". It is now known that barred spirals are at least as abundant as non-barred spirals, and that some galaxies that appear to be non-barred in blue light can appear to be barred when imaged at infrared wavelengths (Eskridge *et al*. 2000).

The existence of non-disk-shaped (and therefore non-spiral) galaxies was at first somewhat controversial. Based on the limited plate material available in his day, Curtis (1918) believed that all galaxies were spiral, and any that did not appear to be spiral on his plates would be found to be spiral when observed with larger telescopes. Hubble, having access to better telescopes, disagreed with this conclusion and believed that genuine non-spiral galaxies existed. Hubble recognized such galaxies as elliptical galaxies, where the luminosity distribution is defined by a regular decline from a bright center to the faint outer regions. Ellipticals were thought to be characterized by no other features but their isophotal shapes, which ranged from round (E0) to a flattening approaching that of disk-shaped galaxies (E7). In fact, Hubble believed the sequence of E galaxy shapes blended smoothly into the domain of disk-shaped galaxies, which he split into two parallel sequences of normal and barred spirals characterized by the degree of central concentration, the degree of resolution of the spiral arms into what were likely to be star-forming regions and the degree of openness of the spiral arms. Hubble (1936) illustrated these features in his famous "tuning fork" of galaxy morphologies (Figure 1.1). Although this view is now obsolete, the tuning fork is still an effective way of binning galaxies into astrophysically meaningful classes.

In stellar astronomy, temporal terms are often used to describe certain kinds of stars. Stars of spectral classes O, B and A tend to be young and are known as "early-type" stars, while those of spectral classes K and M tend to be older and are called "late-type" stars. Those of spectral classes F and G are known as "intermediate-type" stars. Hubble found it convenient to use similar terms for galaxies, calling galaxies on the left part of the tuning fork early-type galaxies and those on the right part late-type galaxies. In general, E and S0 galaxies are said to be early-type galaxies, S0/a and Sa galaxies are called early-type spirals, Sc-Sm galaxies are called late-type spirals and Sab-Sbc galaxies are called intermediate-type spirals. Unlike for stars, no real temporal meaning was to be implied by these terms.

The value of the Hubble classification system, as well as its limitations, can only be appreciated by examining large numbers of galaxies and attempting to classify them within that system. The small number of astronomers who actually did this, such as Sandage, de Vaucouleurs, van den Bergh and Morgan, all saw the need for modifications or even alternative views, which led to major revisions of the system. This article uses images from the EFIGI project (Baillard *et al*. 2011; de Lapparent *et al*. 2011) to illustrate galaxies of different types within the framework of the CVRHS classification system (Buta *et al*. 2015). The classifications are from Buta (2019).

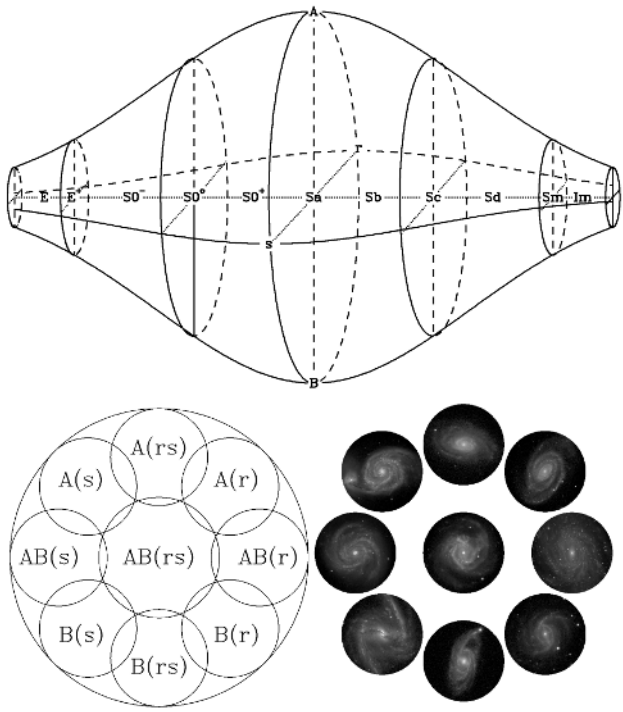

Figure 1.3. *The de Vaucouleurs (1959) revised Hubble–Sandage (VRHS) system of galaxy classification, where the Hubble "tuning fork" has become a classification volume. Top: The VRHS stage sequence. Bottom left: The cross-section of families and varieties. Bottom right: Examples of families and varieties at stage Sbc (from Buta et al. 2007)*

The basic outline of the HS system (Sandage 1961) is depicted in Figure 1.2 and that for the VRHS system is depicted in Figure 1.3. In the HS system, Sandage added the (r) and (s) subtypes, which are also used in the VRHS. The HS system still depicts galaxy morphology as a "tuning fork", but is more complicated than Hubble's original tuning fork (Figure 1.1). In the VRHS, the tuning fork is replaced with a classification volume whose long axis is the stage (E..S0..Sa, Sb..Im, etc.), and whose short axes are the family (SA, SAB, SB) and the variety [(s), (rs), (r)]. The use of "SAB" to denote galaxies having a bar of intermediate apparent strength and "(rs)" for partial inner rings (pseudorings) are major hallmarks of the VRHS and CVRHS systems. Not depicted in the volume are outer rings, large structures about twice the size of a bar in barred galaxies and nuclear rings, much smaller structures about one-tenth the size of a bar in barred galaxies. The appearance of the volume with a broad middle section

and narrower ends is intended to depict how the diversity of families and varieties varies with stage. The greatest diversity is found near stage S0/a, while the diversity diminishes by stages S0 and Im either because bars become difficult to recognize or because rings are simply not present.

The CVRHS is defined by the same kind of classification volume as the VRHS, but with a more finely detailed division into various subtypes. Figure 1.4 shows a cross-section of types through any CVRHS stage from S0° to Sm. The arrangement of families and varieties is the same as in the VRHS, except that de Vaucouleurs' vision of continuity is carried further with the use of *underline notation* that he had applied mainly in his 1963 paper, "Revised Classifications of 1500 Bright Galaxies". The family sequence became SA, SAB, SAB, SAB, SB and the variety sequence became (s), (rs), (rs), (rs), (r). However, in order to recognize outer and nuclear rings in the system, the CVRHS system denotes the presence or absence of an inner feature as the "inner variety", the presence or absence of an outer feature as the "outer variety", and the presence or absence of a nuclear feature as the "nuclear variety". The term "inner feature" now refers to inner rings and lenses, not just inner rings, and the same is true for outer and nuclear features (the latter also including nuclear bars). The recognition of outer pseudorings (R′) is also one of the hallmarks of the VRHS and CVRHS systems. The central subtype in Figure 1.4, (R)SAB(rs,nr), is meant to convey the generalization of VRHS varieties to include inner, outer and nuclear varieties.

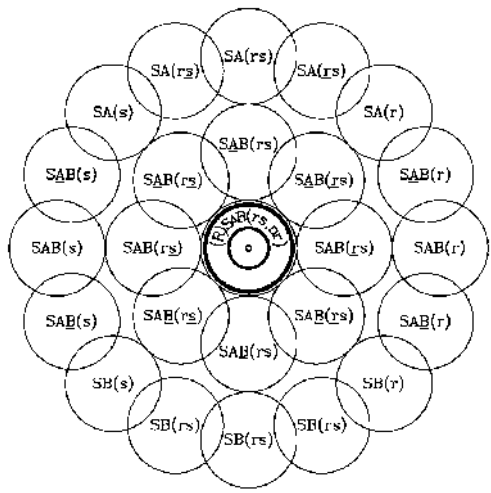

Figure 1.4. *A cross-section through the CVRHS system of families and varieties including the de Vaucouleurs (1963) underline notation. The central "cell" is meant to extend the concept of galactic varieties to outer and nuclear features, as well as additional inner features such as lenses*

de Vaucouleurs (1963) also introduced the underline notation for stages, as in SA(s)ab, which means "closer to Sb than to Sa". Although this notation can be applied directly as for families and inner varieties, it has appeared mainly in classifications based on averages of multiphase (or repeat) efforts designed to check for consistency (e.g. Buta *et al*. 2015). This usage of underlines for stages, families and varieties considerably increases the number of "cells" in the CVRHS as compared to the VRHS, and one may well question whether some of these cells might not have any entrants. Buta (2019) showed that for the EFIGI sample, the cells of the CVRHS system are roughly evenly occupied among late S0s and early-type spirals, but not among later-type spirals. This means the classification volume lacks the symmetry depicted in Figure 1.3.

In the following sections, the different types of galaxies are described in more detail.

1.3. Elliptical galaxies

For more than two decades, elliptical galaxies were the subject of the most intense extragalactic research, spawning many meetings and research papers that underscored how deceptive the simple appearance of these galaxies is. When studied in detail both photometrically and spectroscopically, it becomes clear that the history of ellipticals is likely very complex. The main issues examined in detail are as follows: isophote shapes and orientations; characteristics of luminosity profiles; the presence of dust, rings, and peculiar structures; how low-luminosity ellipticals connect to high luminosity ellipticals; and the characteristic scaling relations between measured quantities such as physical size, surface brightness and central velocity dispersion.

The VRHS system as depicted in Figure 1.3 interprets E galaxies in terms of two stages: E and E^+. A normal elliptical (E) shows a smooth decline in brightness as a function of galactocentric distance, with no inflections or other apparent structure. Type E^+ galaxies are considered as "late" ellipticals showing some traces of structure. The structure can be in the form of a subtle lens, a feature that when more apparent is seen to have a shallow brightness gradient interior to a sharp edge (Sandage 1961; Kormendy 1979). In the Third Reference Catalogue of Bright Galaxies (RC3; de Vaucouleurs *et al*. 1991), the E^+ classification was also applied to brightest cluster members having a shallow brightness gradient (or an apparent extended envelope) in the outer regions. In the Morgan (1958) classification system, such objects are classified as type cD. Examples of E and E^+ galaxies are shown in Figures 1.5 and 1.6. Other aspects of E galaxy morphology include the following:

Disky versus boxy isophotes: The shapes of E galaxy isophotes carry important clues to their history. Kormendy and Bender (1996) noted how Hubble's main E

galaxy classification criterion, the apparent flattening (as in, e.g. E3), had little physical significance, being determined mainly by how a galaxy is viewed. Very few ellipticals are recognized as being more flattened than E4. NGC 4623 in Figure 1.5 is as close as any real galaxy comes to being a genuine E7. Nevertheless, it shows a faint trace of a thin disk (section 1.5).

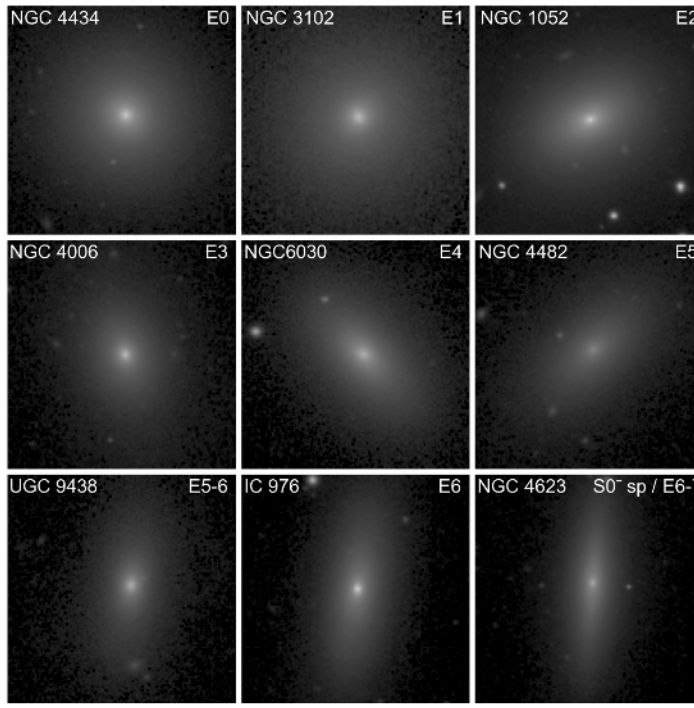

Figure 1.5. *Examples of elliptical galaxies ranging from round in apparent shape (E0) to fairly elongated (E6). Sandage and Bedke (1994) considered NGC 4623 (lower right frame) to be a possible example of a genuine E7 galaxy. Very few ellipticals are more flattened than E4*

Capaccioli (1987) noted two families of elliptical galaxies at a time when any trace of a disk component in a galaxy classified as type E was taken to mean that the galaxy was a misclassified S0 galaxy. Kormendy and Bender (1996) proposed a reclassification of ellipticals into disky and boxy categories based on the sign of the $\cos 4\theta$ relative Fourier deviation from perfectly elliptical isophotes. If the relative amplitude of this term is positive, the isophotes are said to be cuspy (or "disky"), but if negative, the isophotes are boxy. Cuspy isophotes are interpreted as indicating the presence of a subtle disk component, likely to be made of accreted material. Boxy

isophotes are also thought to be indicative of interactive history. If an E galaxy is disky, it is classified as type E(d), while if an E galaxy is boxy, the type is E(b). The distinction of these subcategories can depend on how we are viewing the structures. For example, if the subtle disk in an E galaxy is oriented more nearly face-on rather than edge-on, then the isophotes will not necessarily show a cuspy shape. Both boxiness and diskiness are favored to be seen in the edge-on view. Several examples are shown in Figure 1.7. The CVRHS adopts the E(b) and E(d) terminology of Kormendy and Bender (1996) when these distinctions are obvious in a visual inspection of images.

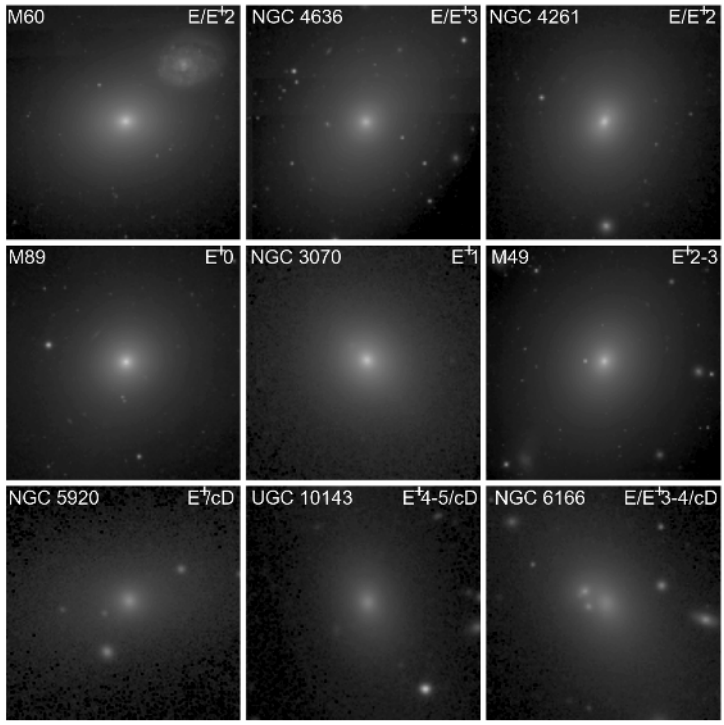

Figure 1.6. *E^+ galaxies are generally elliptical galaxies with very subtle traces of structure, usually in the form of a lens, a feature with a shallow brightness gradient interior to a sharp edge. Lenses are more prominent in S0 galaxies. The bottom row shows three brightest cluster members that are best interpreted as Morgan cD (supergiant) galaxies but which have also been considered E^+ galaxies by de Vaucouleurs*

Isophote twisting: Isophote twisting, where the ellipticity and position angle of the major axis of the isophotes of an E galaxy change systematically with increasing

radius, is thought to be the principal evidence favoring triaxial intrinsic shapes (e.g. Fasano and Bonoli 1989). In a triaxial galaxy, there are three principal axes, each having a different radial scale-length. This highlights how the *observed* ellipticity of an E galaxy cannot be interpreted as easily as that of a disk-shaped galaxy. There is also the possibility, as noted by Nieto (1988), that some isophote twisting in E galaxies is due to an incipient bar structure in a very "early" SB0 galaxy. Tsatsi *et al*. (2017) detected evidence of prolate rotation in eight early-type galaxies, again supporting the idea of triaxial shapes.

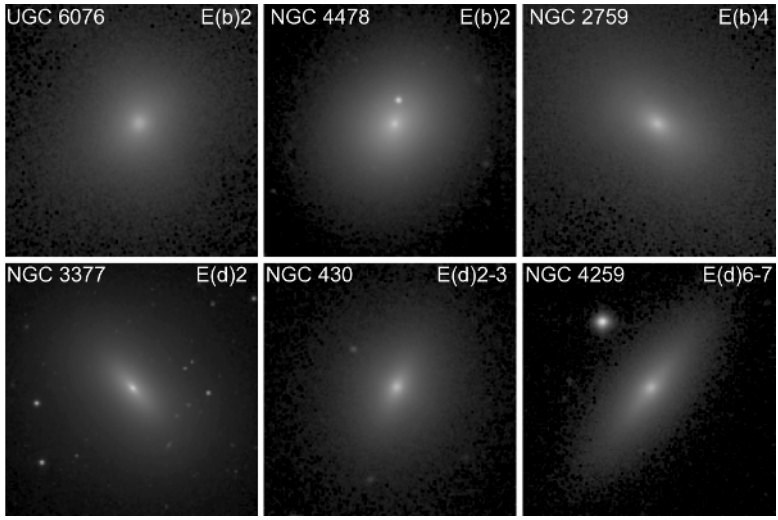

Figure 1.7. *Examples of disky and boxy elliptical galaxies. Generally, the disky/boxy nature of E galaxy isophotes can only be determined with detailed isophotal ellipse fits. The examples illustrated here are more obvious cases that can be distinguished in color displays of the images*

Dust and gas: The presence of interstellar dust and gas in E galaxies is a likely indicator of interaction/merger history (Schweizer 1987). The orientations of planar dust lanes may be tied to the likely triaxial structure of ellipticals. This follows from the presence of *minor axis* dust lanes, where the dust appears along the short apparent axis of the isophotes (Bertola and Galletta 1978). In disk-shaped galaxies, the planar dust lane always appears parallel to the apparent major axis. In general, minor, major and intermediate axis dust lanes are found in E and S0 galaxies. Examples are shown in Figure 1.8. In the CVRHS system, dust-lane Es are specified as E (dust-lane).

Figure 1.8 also includes the peculiar example of NGC 4459, where a small dusty ring, here recognized as a nuclear ring, is found. Although the presence of such a

feature would normally warrant a classification of SA(r)0^+ (Buta *et al*. 2007), the ring is clearly a small disk embedded in a much larger elliptical galaxy.

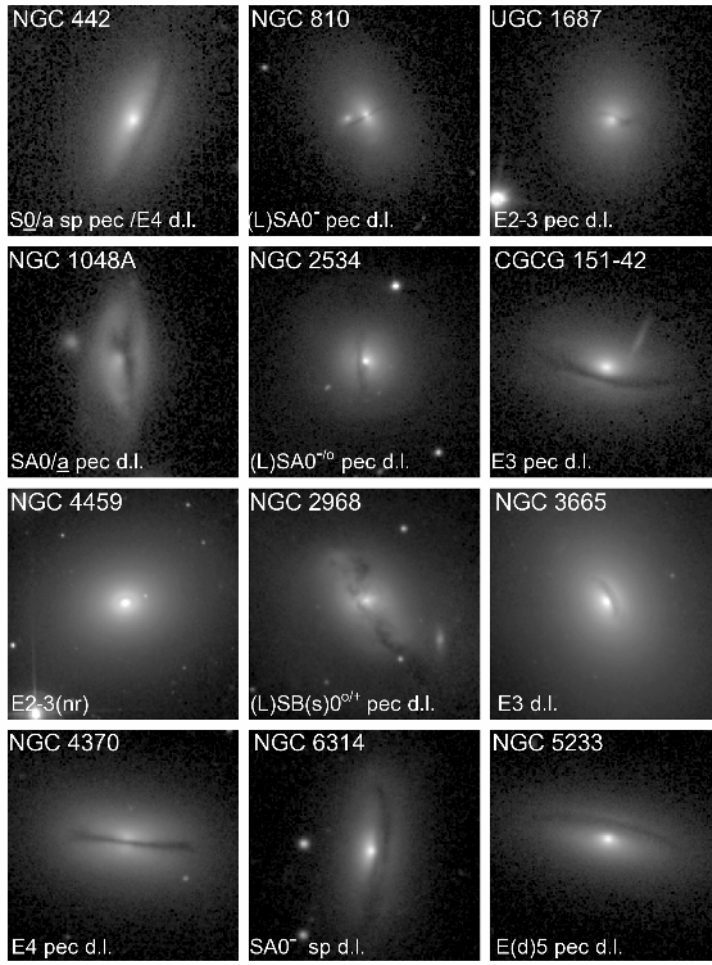

Figure 1.8. *Twelve examples of dust-lane (d.l.) early-type galaxies, including ellipticals and S0s. Major axis (e.g. NGC 442, 4370 and 6314) and minor axis (e.g. NGC 810) cases are included*

Luminosity profiles: de Vaucouleurs (1948) first recognized the well-known "$r^{\frac{1}{4}}$ law" for ellipticals, and for a while it was generally thought that this characterized the luminosity distributions of all E galaxies. When the Sérsic (1968) $r^{\frac{1}{n}}$ approach was used (e.g. Huang *et al*. 2013 and references therein), it became clear that $n = 4$

only characterized the more luminous ellipticals (see review by Graham 2013). Lower luminosity ellipticals have lower values of n. Other aspects of luminosity profiles include the distinction between "core Es", which have a flat central profile, and "power-law Es", which have a central cusp (Kormendy and Bender 1996).

The fundamental plane of E galaxies: Elliptical galaxies are characterized by a well-defined interconnectedness of their physical parameters. In the three-dimensional space defined by the parameters R_e, the effective radius that transmits half the total luminosity; I_e, the average surface brightness within this radius; and σ_o, the central velocity dispersion, an important characteristic emerges. The correlations between these three parameters of elliptical galaxies define what has come to be known as the "fundamental plane" (Kormendy and Djorgovski 1989). The plane tells us that larger E galaxies tend to have lower average surface brightness than smaller E galaxies, and that more luminous E galaxies have higher central velocity dispersion than do lower luminosity E galaxies.

1.4. Spiral galaxies

The spiral structure of galaxies was discovered more than 170 years ago. The subtle patterns were first detected in 1845 with the world's largest telescope at the time, the "Leviathan of Parsonstown" located in central Ireland. William Parsons, the Third Earl of Rosse, visually saw the spiral arms of the "Whirlpool Galaxy" M51 with his newly built 72-inch speculum metal reflector. In the parlance of 19th Century astronomy, M51 was called a "nebula", not a galaxy, although the general view at the time was that most or all nebulae were distant systems of stars like the Milky Way ("Island Universe" hypothesis). Parsons built the Leviathan partly to test this idea. The discovery of spiral structure added mystique to the nebulae, and led to alternative ideas as to what the nebulae actually were. It would be nearly a century after Parsons' discovery that any serious understanding of the nature of spiral structure would be achieved (section 1.11).

Spiral galaxies are generally two-component systems consisting of a bulge and a disk. Although at one time bulges were thought to be generally less flattened components than disks, it is now clear that bulges include a mix of dissimilar structures, such as spheroidal "classical" bulges, highly flattened "pseudobulges" (Kormendy and Kennicutt 2004) and "boxy/peanut" bulges, the latter thought to be due to edge-on views of bars (e.g. Lutticke and Dettmar 1999).

The classification of spirals is generally based on a rough correlation between the degree of central concentration and the character of the spiral arms. Hubble had noticed that galaxies with tightly wrapped, relatively smooth arms tended to have bright central bulges, while galaxies having open, relatively patchy spiral arms tended to have very small bulges. Hubble (1926) called the former cases Sa galaxies and the

latter cases Sc galaxies, with Sb galaxies being intermediate between the two types. This observation set the stage for galaxy classification for nearly a century. However, the correlation works best for non-barred galaxies. It is poorer for barred galaxies that, even in cases with smooth, tightly wrapped arms, can have very small bulges. An example is NGC 3351, type SBb, which has a very small bulge in the center of a bright nuclear ring (Buta *et al*. 2007). Because of such inconsistencies, Sandage (1961) advocated basing spiral stage classifications (i.e. Sa, Sb, etc.) mainly on the appearance of the spiral arms.

Figure 1.9 shows a full CVRHS stage sequence for non-barred galaxies from stage S0° to stage Sm, that is, from the intermediate S0 stage (Figure 1.3) to the latest stage on the spiral sequence. The spiral sequence begins with the stage S0/a, which is considered to be a transition type between S0s and spiral galaxies. Type S0/a is a legitimate type in the sense that it is easily recognized and the continuity that de Vaucouleurs envisioned seems well represented by the type. Nevertheless, this apparent continuity does not necessarily imply that all S0s are correctly placed in the Hubble (1936) "tuning fork". The stage generally begins with pseudorings made of tightly wrapped spiral structure as in NGC 809. In the CVRHS classification, stage S0/a is closer to S0 than to Sa, while S0/a is closer to Sa than to S0.

The sequence for non-barred galaxies in Figure 1.9 shows the rough correlation between central concentration and stage. Bulges are most prominent at stages Sbc and earlier, and are least prominent at stages Sc and later. The sequence shows well how arms are smooth at stage Sa and knotty, well-resolved, more open features at stage Sc. Intermediate stages are as well defined as regular stages: Sab galaxies often resemble Sa galaxies but with a greater degree of resolution into star-forming regions; Sbc galaxies typically have the bulge of an Sb galaxy in a disk with Sc arms; Scd is recognized as an Sc galaxy with only a trace of central concentration; and Sdm galaxies are typically bulge-less asymmetric systems with an offset bar and one spiral arm longer than the other. Similar underline stages (e.g. Sab. Scd) are used throughout the CVRHS sequence (de Vaucouleurs 1963).

Figure 1.10 shows the same kind of stage sequence for barred galaxies. Initially, Hubble (1926) believed that non-barred galaxies were the "normal" form of spirals, with perhaps maybe 20% of the spirals being barred. He nevertheless envisioned barred spirals as falling on a sequence parallel to that of non-barred spirals. In the Hubble Atlas of Galaxies, Sandage (1961) smoothly connects non-barred and barred S0s with the non-barred and barred spiral prongs, respectively, which is also true for the VRHS and the CVRHS systems. The same kinds of types are recognizable among barred spirals as among non-barred spirals. However, Figure 1.10 shows the small bulge effect in early-type barred spirals, an example being NGC 5610 whose smooth arms wrap into an outer pseudoring but whose bulge is no more prominent than that in an Sc galaxy.

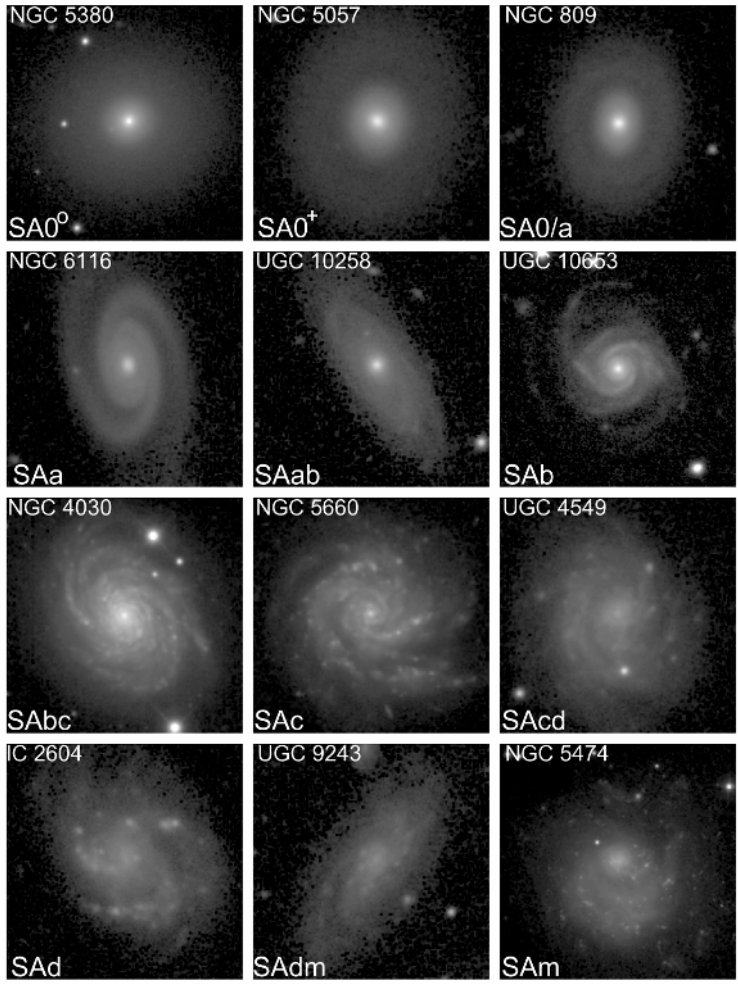

Figure 1.9. *A sequence of stages for non-barred galaxies in the VRHS/CVRHS system*

The bars of spiral galaxies: As already noted in section 1.2, the CVRHS classification of bars utilizes five categories, SA, SAB, SAB, SAB and SB (de Vaucouleurs 1963), in a sequence of increasing visual bar strength (Figure 1.11). The classification is based on the length, contrast and axis ratio of the bar or bar-like feature. Although leading dust lanes are not a classification criterion for bars, such lanes are often seen in barred spirals of types S0/a to Sbc and could impact the apparent bar strength. Based on CVRHS classifications, the bar fraction is about 50%

for SAB, SA<u>B</u> and SB cases, but increases to 67% if S<u>A</u>B is included (Buta *et al*. 2015; Buta 2019). The cosmological significance of the bar fraction is discussed by Sheth *et al*. (2008).

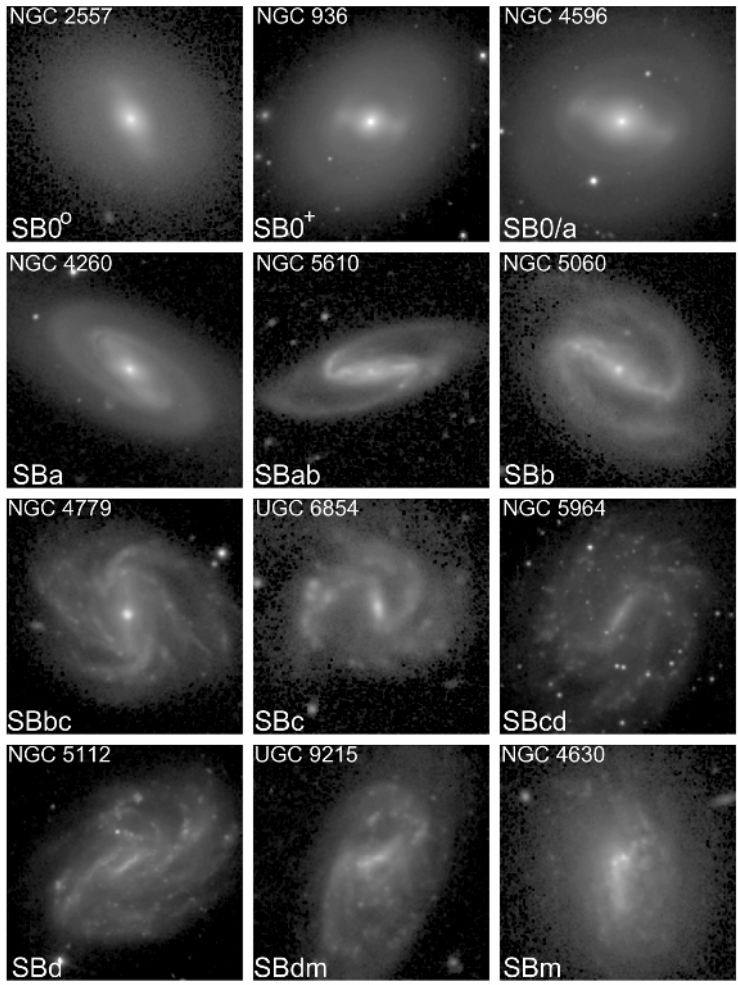

Figure 1.10. *A sequence of stages for barred galaxies in the VRHS/CVRHS system*

There are additional aspects of bars recognized in CVRHS classifications. Most bars are regular bars, the kinds of features seen in classic barred spirals like NGC 1300 or NGC 1365. Others are "ansae-type" bars, where the bar appears to have "handles" or enhanced spots at the ends (Martinez-Valpuesta *et al*. 2007). Several examples are shown in Figure 1.12, which are classified using the symbols SB_a or

SAB_a. In some cases, the appearance of ansae-type bars suggests a regular bar in the process of actual dissolution. On the other hand, Athanassoula *et al*. (2016) have recently used numerical simulations to show that ansae could form in the disk-shaped remnant of the merger of two spiral galaxies. Another aspect of bar classification comes from box/peanut bulge galaxies. A box/peanut bulge galaxy is generally an edge-on disk-shaped galaxy where the bulge has boxy isophotes and has the look of an "X" pattern crossing the center. One of these is shown in Figure 1.12 and several others are shown in Figure 1.13 (bottom row). The appearance of a boxy/peanut bulge can depend on whether the bar is viewed end-on or broadside-on. The X is believed to be a result of the line of sight view through vertical resonant bar orbits (e.g. Abbott *et al*. 2017). The classifications SB_x and SAB_x are used for boxy/peanut bulges. In some cases, both a boxy/peanut bulge and ansae occur in the same system (as in NGC 5445; Figure 1.12). In such cases, the classification is SB_{ax} or SB_{xa}.

Although the CVRHS bar family classification can be consistently applied, it is still a visual judgment and is not the most effective way of quantifying bar strength. It is also technically based on blue light images (the historical waveband of galaxy classification) where the appearance of the bar may be affected by dust and star formation. More quantitative approaches to bar strength include the maximum ellipticity in the bar region, the maximum relative $m = 2$ Fourier intensity amplitude $A_2 = (I_2/I_0)_{\max}$ and the ratio of the maximum tangential force to the mean radial force in the bar region, all based on near-infrared images (e.g. Combes and Sanders 1981; Buta and Block 2001; Buta 2012). Garcia-Gómez *et al*. (2017) describe the application of a two-dimensional Fourier transform technique to more reliably characterize the strengths of bars in disk galaxies.

Inner varieties: The inner variety of any disk-shaped galaxy refers to the presence or absence of an inner ring (Sandage 1961). If an inner ring is present, the inner variety is (r). In a spiral, the spiral structure breaks from near the location of the inner ring. The inner variety is (s) if there is no inner ring and the spiral structure either winds all the way to near the center of the galaxy or breaks directly from the ends of a bar. In many galaxies, a partial inner ring made of tightly wrapped spiral structure is seen. As noted in section 1.2, such "pseudorings" are recognized by the symbols (rs) in the variety sequence: (s), (r$\underline{\text{s}}$), (rs), ($\underline{\text{r}}$s), (r), where the underlines denote the dominant characteristic. Examples of these morphologies are shown in the upper row in Figure 1.14.

Inner rings are most common in barred galaxies, but also appear in non-barred galaxies. Some non-barred galaxies with rings could be evolved remnants of an earlier barred phase, owing to the possibility that bars may dissolve in much less than a Hubble time due to a buildup of the central mass concentration (Norman *et al*. 1996).

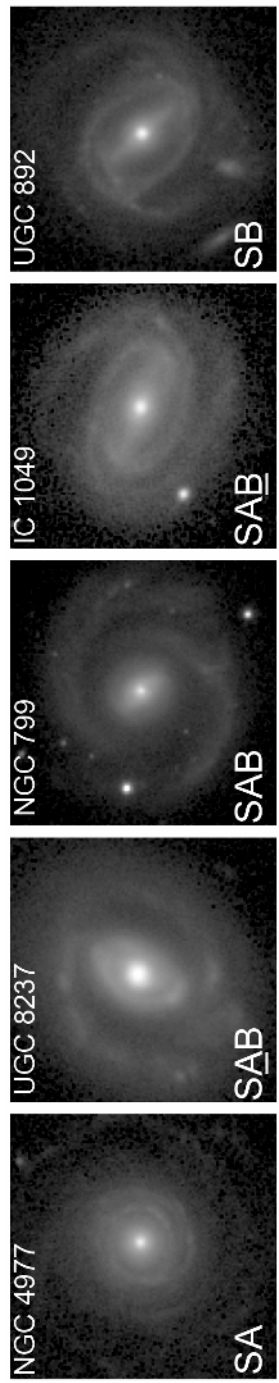

Figure 1.11. *A sequence of increasing apparent bar strength*

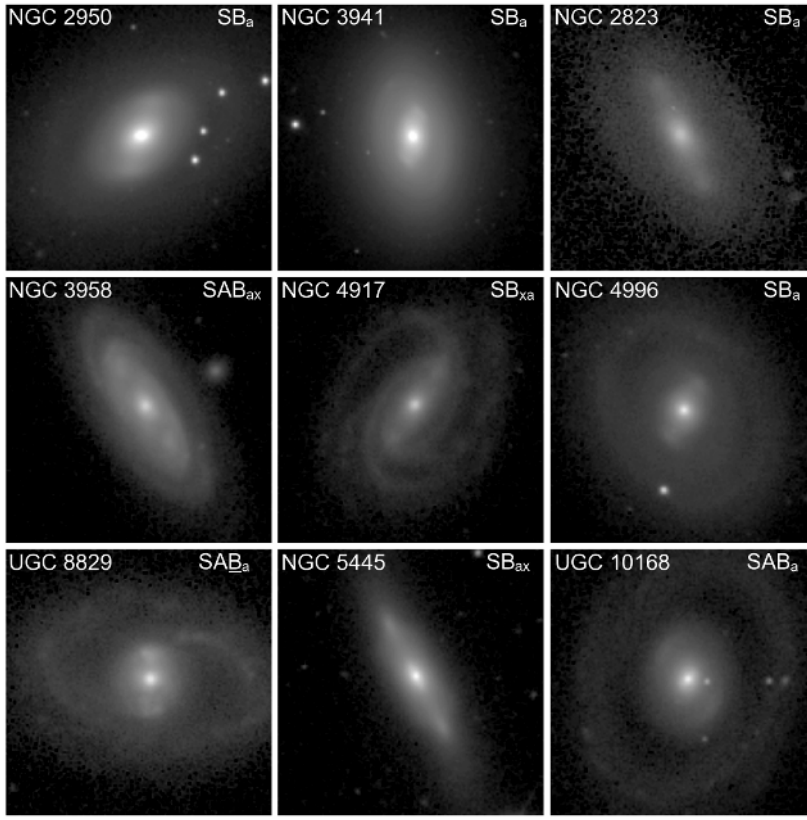

Figure 1.12. *Bars showing enhanced "handles", or ansae. The features appear in spot, linear or curved form*

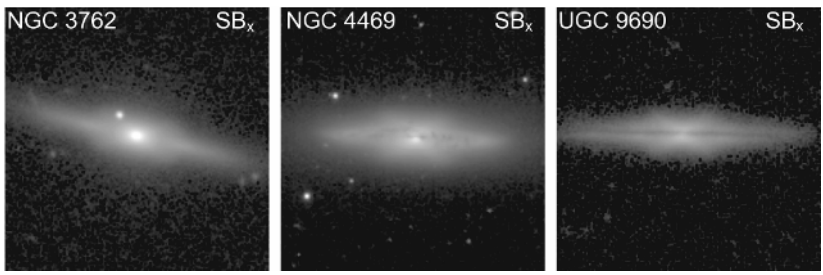

Figure 1.13. *Three edge-on galaxies showing boxy/peanut-type bulges*

A different inner variety sequence is sometimes applicable. As noted in section 1.3, early-type galaxies often show inner lenses, which are features located in the same place where an inner ring would be seen. If a bar is present, the bar usually fills the inner lens in one dimension (Kormendy 1979). The symbol for an inner lens is (l) and that for an inner ring-lens is (rl). These are used in the sequence: (r), (rl), (rl), (rl), (l). Examples of these morphologies are shown in the bottom row of Figure 1.14. In some cases, the inner variety is r′l, meaning an inner pseudoring-lens. In an actual classification, the inner variety is in parentheses between the family and the stage [as in, e.g. SB(r)b, SAB(rs)cd, SA(l)0/a, etc.].

The relation between inner rings and inner lenses is unclear. One possibility is that an inner lens is a highly evolved inner ring. This might account for the existence of inner ring-lenses (rl), which appear to be low contrast inner rings. However, Kormendy (1979; see also Bournaud and Combes 2002; Gao *et al*. 2018) proposed another interpretation: that inner lenses represent dissolved bars. Bar dissolution is possible because the presence of a bar not only heats the disk component, but also causes resonance effects that force stars onto orbits that do not support the bar. An example of the latter is the formation of a *nuclear bar*, which is a small secondary bar that forms inside a primary bar. Such features are recognized with the symbol (nb) in the CVRHS classification system, and are often significantly misaligned with a primary bar if present.

An interesting aspect of inner rings and lenses is that the former are most common in barred galaxies, but the latter are most common in non-barred galaxies. A possible reason for this is that bar dissolution could leave behind a lens that was formerly the inner part of the bar, called a *barlens* (Laurikainen *et al*. 2013). A barlens [symbolized by (bl)] is generally the roundish, inner component of a bar that often is mistaken for a classical bulge. Examples are shown in Figure 1.18. Athanassoula (2016) interprets barlenses as the three-dimensional inner sections of bars that appear as boxy/peanut bulges in the edge-on view. The ends of the bar are much flatter than this inner section. In general, the boxy character of these inner sections is not very evident in the near face-on view. However, in some bars, an inner boxy zone is seen even in a lower inclination view (examples: NGC 7020, IC 4290, IC 5240; Buta *et al*. 2007).

Another interesting aspect of inner rings is that these features have a wide range of intrinsic shapes (deprojected minor-to-major axis ratio 0.5 to 1.0; Buta 2019) and are often regions of intense star formation. The distribution of star formation in inner rings is sensitive to this range: the more elongated the ring, the greater the concentration of HII regions around the major axis points (Crocker *et al*. 1996; Grouchy *et al*. 2010). The effect is especially evident in cuspy-shaped inner rings, of which NGC 6782 is the best example (Lin *et al*. 2008). It is also seen in NGC 3081 (Buta and Purcell 1998).

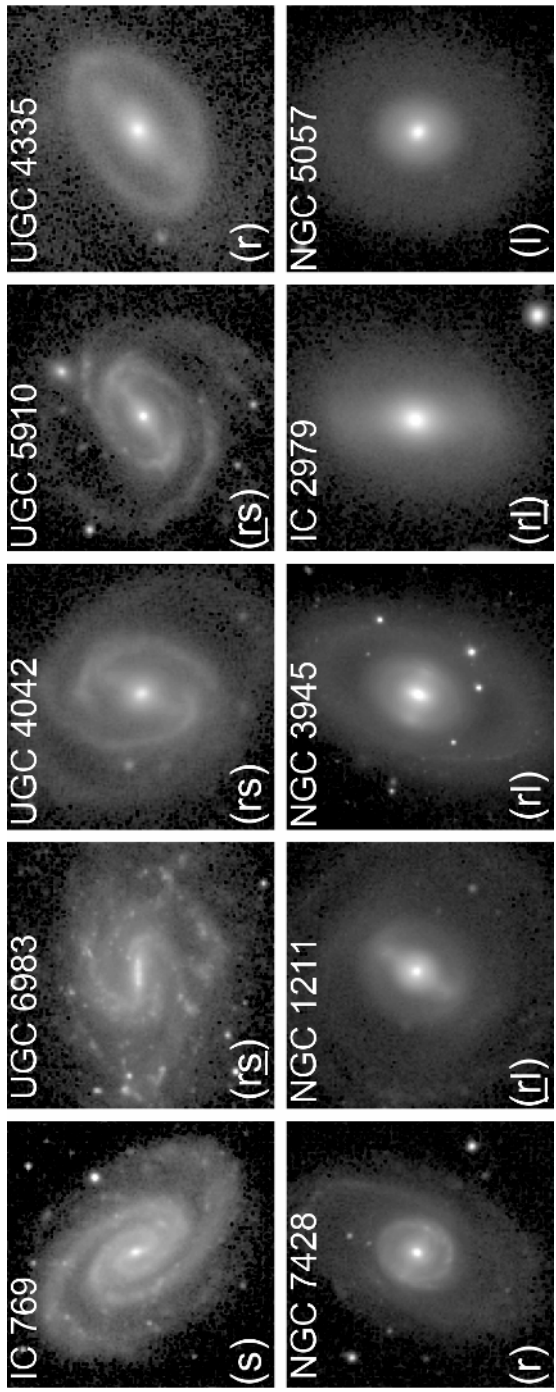

Figure 1.14. *Examples of different inner varieties*

Nuclear varieties: The nuclear variety of a disk-shaped galaxy refers to the presence of nuclear structure, usually in the form of a nuclear ring (nr), nuclear pseudoring (nr′), nuclear spiral (ns), nuclear bar (nb), nuclear lens (nl) or nuclear ring-lens (nrl). The features tend to be small and therefore are recognizable mainly in nearby galaxies. The features also have a wide range of linear diameters, from a few hundred pc to nearly 5 kpc (Comerón *et al*. 2010). In some cases, a nuclear ring is crossed by a nuclear bar. Figure 1.15 shows several examples of spiral galaxies having a nuclear ring. In a CVRHS classification, the nuclear variety appears with the inner variety. For example, NGC 3081 is classified as $(R_1R'_2)$SAB(r,nr,nb)0/a, where the inner/nuclear variety is (r,nr,nb). Knapen (2005) determined that $21\pm5\%$ of spiral galaxies have nuclear rings or related features.

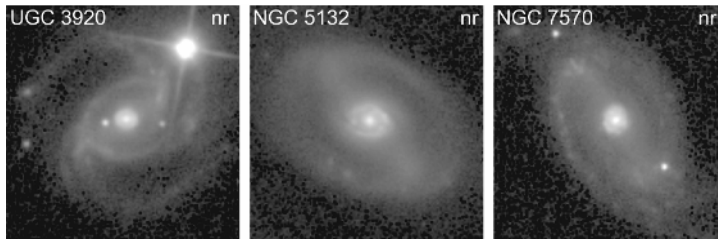

Figure 1.15. *Examples of spiral galaxies having a nuclear ring*

Outer varieties: Just as inner varieties refer to inner rings and lenses mainly, outer varieties refer to outer rings and lenses. While a typical inner ring or pseudoring in a barred galaxy has about the same size as the bar, the typical outer ring is about twice the size of the bar. Outer features are typically more diffuse than inner features, and of lower surface brightness. The main types of outer features include outer rings (R), outer pseudorings (R′), outer lenses (L), outer ring-lenses (RL) and outer pseudoring-lenses (R′L). An example of each of these, including a doubled outer ring case (RR), is shown in Figure 1.16. In all cases, the outer feature classification is positioned ahead of the family classification, as in (RL)SA(l)0° or (R′)SB(rs)ab.

In spiral galaxies, outer features tend to be pseudorings or pseudoring lenses. The best-defined outer rings tend to be found in $S0^+$ or S0/a cases. The galaxies NGC 2859 (Figure 1.16) and 3945 (Figure 1.14) are two of the best examples of outer rings. Both are classified by Buta (2019) as (R)SA$\underline{B}_a$(rl,bl,nb)0^+, meaning they are "late" S0s. A typical outer pseudoring is seen in NGC 5610, type (R′)SB(s)ab (Figure 1.10). Outer pseudorings are much more common than outer rings.

Among outer features are the resonant subclasses, that is, features that strongly resemble the kinds of resonance rings that form in numerical simulations of barred galaxies, specifically the models of Schwarz (1981) and Byrd *et al*. (1994). Figure 1.17

shows examples of the R_1, R_1', R_1R_2' and R_2' subclasses of outer rings and pseudorings. The way to recognize these features is described by Buta (2017b). The outer resonant subclasses constitute only a small fraction of outer features. Most disk-shaped galaxies do not have an outer feature, but among the ones that do, outer pseudorings of type R' (excluding the resonant subclasses) are most abundant. The formation of rings has been reviewed in Buta and Combes (1996) and is discussed further in section 1.12.

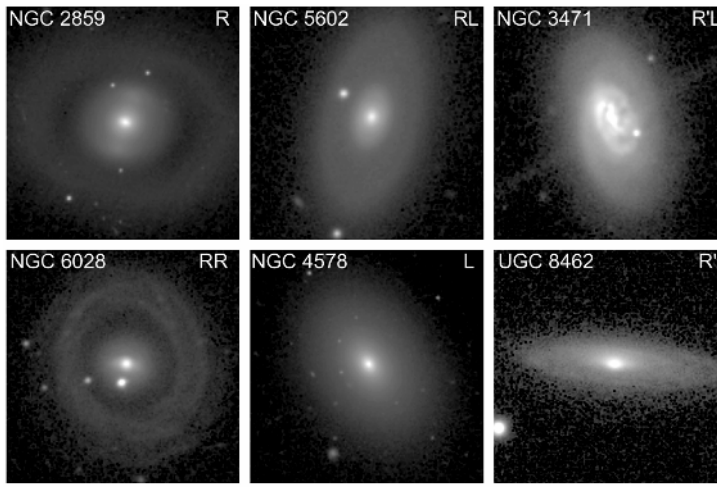

Figure 1.16. *Examples of different types of outer features. The feature type is in the upper right of each frame*

1.5. S0 galaxies

S0 galaxies are generally viewed as "armless" disk galaxies. Once referred to as "lenticulars" because of their double convex lens-like appearance in the edge-on view, S0s first appeared as a galaxy type in Hubble's 1936 book, *The Realm of the Nebulae*, where he presents his "tuning fork" depiction of his system (Figure 1.1). Although ellipticals, normal spirals and barred spirals were the main types recognized in Hubble's original 1926 classification system, the possibility of S0 galaxies was raised even then. Something was puzzling about the original system in that Sa galaxies usually had fully developed arms while SBa galaxies did not. To account for this, Hubble hypothesized the existence of a class of disk-shaped galaxies lacking spiral arms. He placed these at the juncture of the "tuning fork", where the most flattened-looking E galaxies link with the two parallel sequences of spiral galaxies. As Hubble increased his database of photographic images of "nebulae", real examples of the hypothesized group of armless disk galaxies were found. Hubble was working on a revision to his system but died before publishing it. Sandage (1961) used Hubble's notes to make the revision: S0s were interpreted in terms of two

sequences of three "normal" stages: $S0_1$, $S0_2$ and $S0_3$, and three barred stages $SB0_1$, $SB0_2$ and $SB0_3$ (Figure 1.2). The subdivision of non-barred S0s was based on the development of structure such as the appearance of dust lanes, while the subdivision of barred S0s was based on the development of the bar from something very subtle to a more prominent feature.

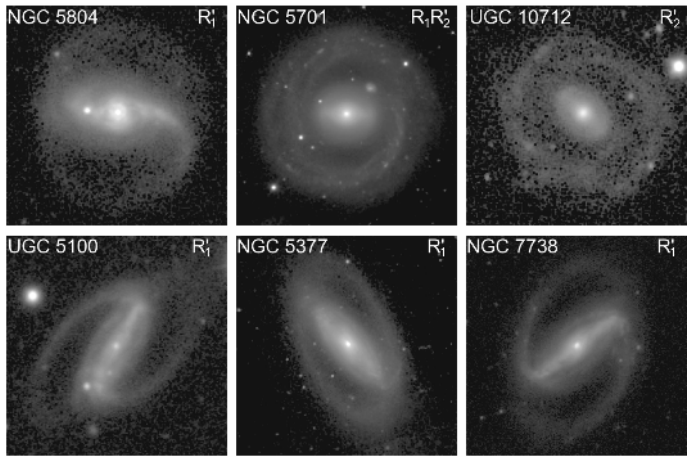

Figure 1.17. *Outer resonant features. The feature type is in the upper right of each frame*

The tuning fork arrangement of galaxy types with S0s included began to be questioned when it was realized that S0s had lower luminosities than Sa or SBa galaxies and thus do not really link smoothly to those parts of the Hubble sequence. This led to the "parallel-sequence" interpretation of S0s, whereby S0s form a sequence parallel to the spirals (not to be confused with the normal/barred spiral prongs of the tuning fork). This interpretation is based on a nurture view that S0s are former spiral galaxies that have been stripped of their interstellar gas and dust through environmental interactions (van den Bergh 1976). On a sequence between spirals and S0s, van den Bergh placed what he called "anemic spirals" or galaxies in an intermediate state of stripping. Real examples of galaxies in such an intermediate state have been found in the Virgo Cluster (Koopmann and Kenney 2004) and the Coma Cluster (Yagi *et al*. (2010).

Figure 1.19 shows several S0 galaxies classified in the CVRHS system. The CVRHS system treats S0s differently from the tuning fork and parallel sequence ideas. Like spirals, S0s are divided into stages, families and varieties (Figure 1.3). The stage for S0s has three subdivisions: $S0^-$, $S0^\circ$ and $S0^+$, a sequence of increasing structure (but not necessarily decreasing bulge to total luminosity ratio, which determines stages along the spiral sequences). Intermediate CVRHS stages from

average multiphase classifications (as in Buta *et al*. 2015 and Buta 2019) are $S0^{-/\circ}$ and $S0^{\circ/+}$.

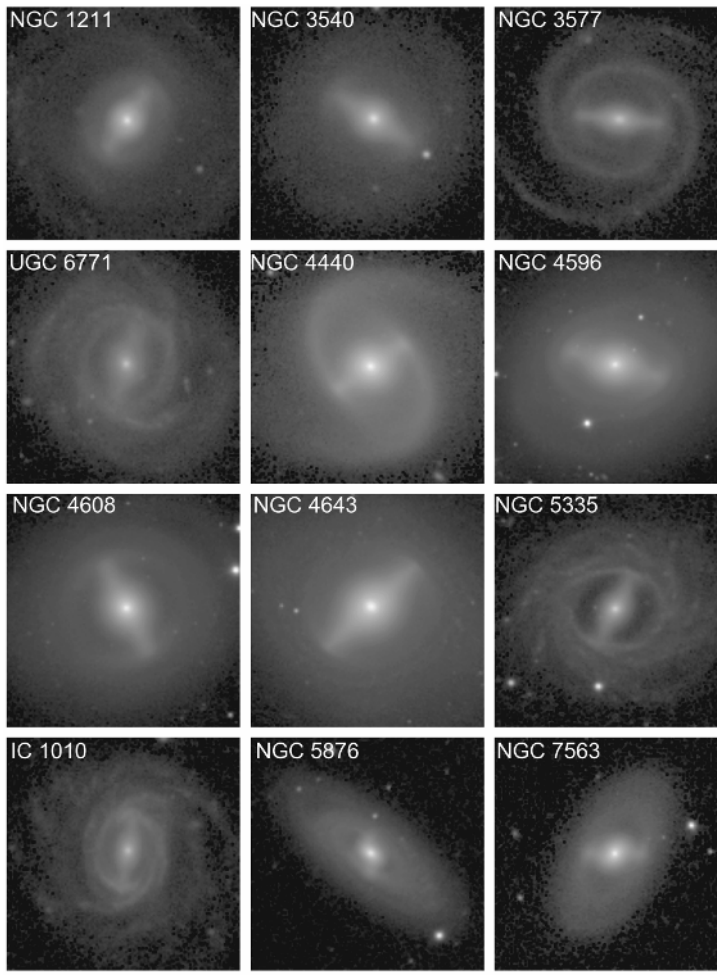

Figure 1.18. *Twelve examples of barred galaxies having a "barlens", which refers to the roundish section inside the bar. Several of these show light deficits around the bar, especially NGC 5335 (Buta 2017b; see also Gadotti and de Souza 2003b; Kim et al. 2016)*

Lenses are common in early S0 galaxies. For example, typical $S0^{-}$ and $S0^{-/\circ}$ galaxies have mostly featureless extended envelopes that often have a subtle outer edge. Such features are classified as outer lenses (L). Faint traces of inner lenses (l) are also seen in such galaxies. As noted in section 1.4, the origin of lenses is uncertain.

Some or most inner lenses are thought to be due to the dissolution of bars (Kormendy 1979), but the existence of outer and nuclear lenses suggests a possible link to the evolution of rings.

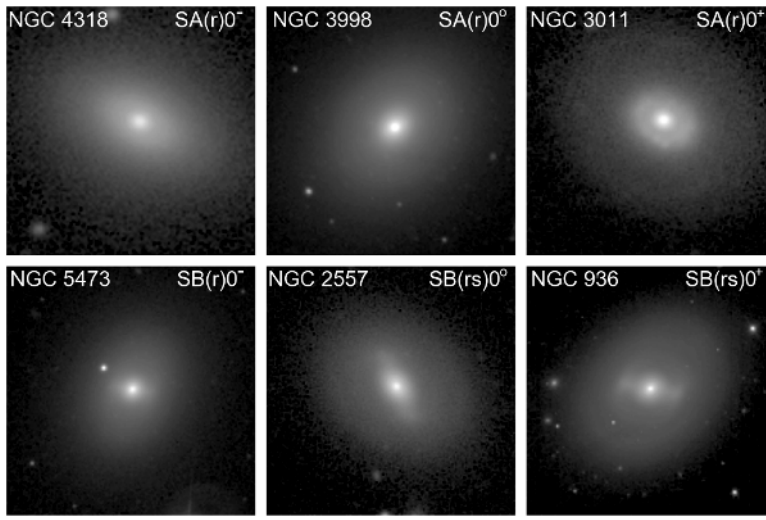

Figure 1.19. *Stage sequences for both barred and non-barred S0 galaxies*

1.6. Magellanic spiral and irregular galaxies

In distance-limited samples of galaxies, Magellanic spirals and irregulars are the most common types of galaxies. Encompassing a wide range of luminosities from dwarfs to giants, Magellanic spirals and irregulars are generally HI rich systems with considerable active star formation. Several examples are shown in Figure 1.20.

The Magellanic Clouds are considered to be examples of SB(s)m galaxies, i.e. extreme late-type galaxies having clear bars but very subtle spiral structure showing a characteristic asymmetry with a single main arm and weaker features (de Vaucouleurs and Freeman 1972). This asymmetry is recognizable even in the nearly edge-on view (Buta *et al*. 2015). The transition stage from Sd to Sm, or Sdm, is also well defined in showing two arms with one much longer than the other. As for Scd and Sd galaxies, Sdm, Sm and Im galaxies are often barred, except for low luminosity dwarfs that may lack the mass required to show such a feature. Non-barred giant late-type galaxies like NGC 5474 show a similar asymmetry to SBm galaxies and can be classified as type SA(s)m.

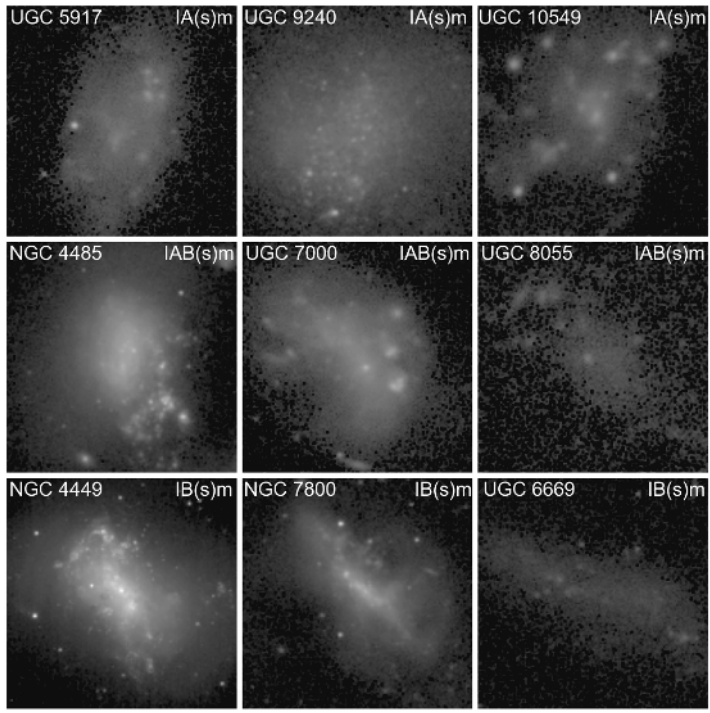

Figure 1.20. *Magellanic irregular galaxies*

1.7. Dwarf elliptical, S0, and spheroidal galaxies

In the environment of the Virgo Cluster, the most common type of galaxy is not an irregular, but what Sandage and Binggeli (1984) called a dwarf elliptical (dE) type. Of nearly 2,000 catalogued galaxies in the Virgo Cluster, Sandage and Binggeli (1984) found that 80% were of this type. A dE galaxy is a low luminosity system with a relatively smooth luminosity distribution that resembles a conventional elliptical galaxy but has a low surface brightness and a luminosity distribution closer to an exponential than to the $r^{\frac{1}{4}}$ law. In some cases, there is subtle structure similar to what is seen in conventional S0 galaxies, and the system is referred to as a dwarf S0, or dS0, galaxy. In either case, the object may be *nucleated*, and if so, the classification is dE,N or dS0,N. In contrast, dwarf spirals, or dS types, are extremely rare.

The exact placement of the dE and dS0 systems within the Hubble tuning fork can be examined by studying the luminosity distributions and investigating scaling relations among elliptical galaxies of all luminosities. Based on such studies,

Kormendy and Bender (2012) concluded that dE and dS0 galaxies are not merely the low luminosity extensions of classical E galaxies, but are *environmentally modified* former irregular and dwarf irregular galaxies. Kormendy and Bender (2012) suggested that all such galaxies be referred to as "Spheroidal" galaxies, and that their existence supports the idea of the van den Bergh (1976) parallel-sequence classification.

In the CVRHS system, the dE and dS0 classification symbols of Sandage and Binggeli (1984) are adopted in the form dE/dS0/Sph or dE/S0,N/Sph. Ann *et al*. (2015) show numerous examples.

1.8. Edge-on galaxies

Edge-on disk galaxies can be more difficult to classify than face-on galaxies, owing to the foreshortening of features such as spiral arms, bars and rings. Nevertheless, the degree of central concentration is often still detectable in spite of heavy planar extinction, and the degree of resolution in the disk can still be used, so that the stage is still discernible (Figure 1.21). Features like inner varieties have to be left out of the classification, leaving types such as Sbc sp, Sd spw, etc. The characteristic "sp" (meaning "spindle-shaped") is only used to single-out edge-on or nearly edge-on disks, and does not imply prolate rotation. A galaxy classified as "spw" is one that shows evidence of disk warping in the edge-on view. Some extreme cases of disk warping are shown in Buta *et al*. (2015).

Embedded disks and thick disks: An embedded disk system is a case where a disk galaxy is embedded within a clear 3D component, usually an E galaxy of low flattening. In a disky elliptical galaxy, classified as type E(d) in the notation of Kormendy and Bender (1996), the presence of a faint disk is inferred from subtle distortions of isophotes. As noted in section 1.3, disky isophotes are detected through positive values of the $\cos(4\theta)$ relative Fourier component of deviations from a perfectly elliptical shape. Embedded disk systems are similar to disky ellipticals, only the disk is much more obvious.

The 3D systems the disks are embedded in may be considered part of the bulge, and the disk may appear to underextend, fill or overextend the isophotes of that system (Buta *et al*. 2015). While disky E systems are best detected when the disk is close to edge-on, more prominent disks need not be so inclined. Figure 1.22 shows several examples. Embedded disks are recognized in CVRHS classification by a notation such as, for example, $S0^-$ sp/E(d)2-3 where the "$S0^-$ sp" part is the spindle-shaped edge-on disk component and the "E(d)2-3" refers to a low flattening E galaxy the disk is embedded within. Obvious embedded disks, where the background spheroidal system has a low flattening, are not common. In general, the flattening of the spheroidal part of an embedded disk system, and the character of the isophotes as boxy or disky, are estimated using a color display of the galaxy's isophotes. In rare cases, the extended

component is boxy rather than cuspy, as in the case of NGC 4638 where the CVRHS type is S0$^-$ sp/E(b)3.

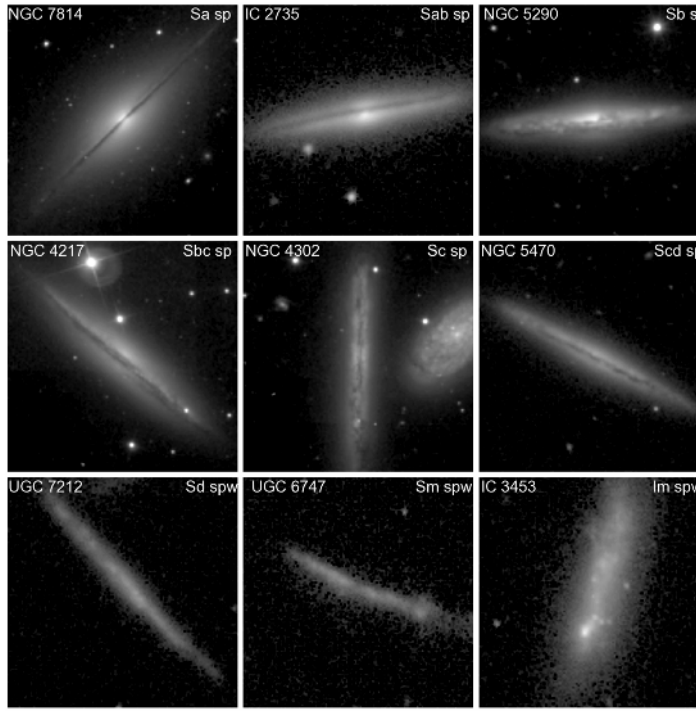

Figure 1.21. *Edge-on galaxies from stage Sa to stage Im. The "sp" stands for "spindle" and is used to characterize the edge-on orientation. If "spw", it means the edge-on disk shows signs of warping*

Most spiral and S0 galaxies do not have dominant classical bulges, but many have a two-component disk: the *thin disk*, which has a vertical scale height of a few hundred pc, and the *thick disk*, which shares the same plane with the thin disk but has a vertical scaleheight of about 1 kpc. Especially in spirals, the two disks can have very different stellar populations, with population I material occupying the thin disk and population II material occupying the thick disk. As for embedded disks, thin and thick disks are recognized in CVRHS classifications by combining a normal stage classification with an E(d) or E(b) classification as in, for example, S0$^-$ sp/E(d)7. In this case, the "S0$^-$ sp" part refers to the thin disk and determines the stage index T of the galaxy. The "E(d)7" part refers to the thick disk, whose apparent flattening and isophotal character (cuspy or boxy) are judged from a color display. Note that thick disks may have cuspy, boxy or perfectly elliptical isophotes, the latter requiring no (d) or (b) added to the classification.

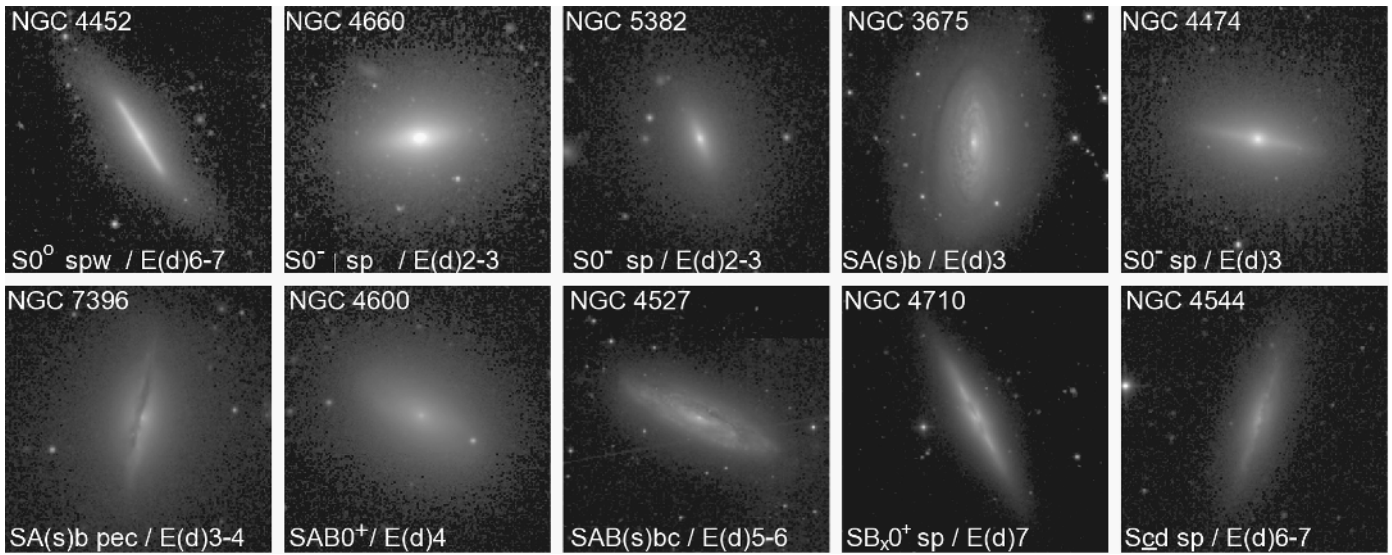

Figure 1.22. *Embedded disks and thick/thin disks. The main embedded disk cases shown are NGC 4660, NGC 5382, NGC 3675 and NGC 4474, and the thick/thin disk examples include NGC 4452, NGC 4527, NGC 4710 and NGC 4544*

1.9. Morphology of interacting and merging galaxies

Interacting and merging galaxies make up about 2–4% of nearby galaxies (Knapen and James 2009) and are often unclassifiable in any standard Hubble-based morphological bins. Figure 1.23 shows several examples, all of which are classified as Pec (merger) in the CVRHS system. Distorted shapes, tidal tails, sharp edges ("shells" or "ripples"; e.g. Schweizer and Seitzer 1988), multiple nuclei, and in some cases enhanced star formation characterize these objects. Although major mergers of two spiral galaxies have been thought to generally lead to an elliptical galaxy as a remnant (e.g. Schweizer 1982), more recent numerical studies have shown that a disk galaxy can also be a remnant of such mergers (Athanassoula *et al*. 2016).

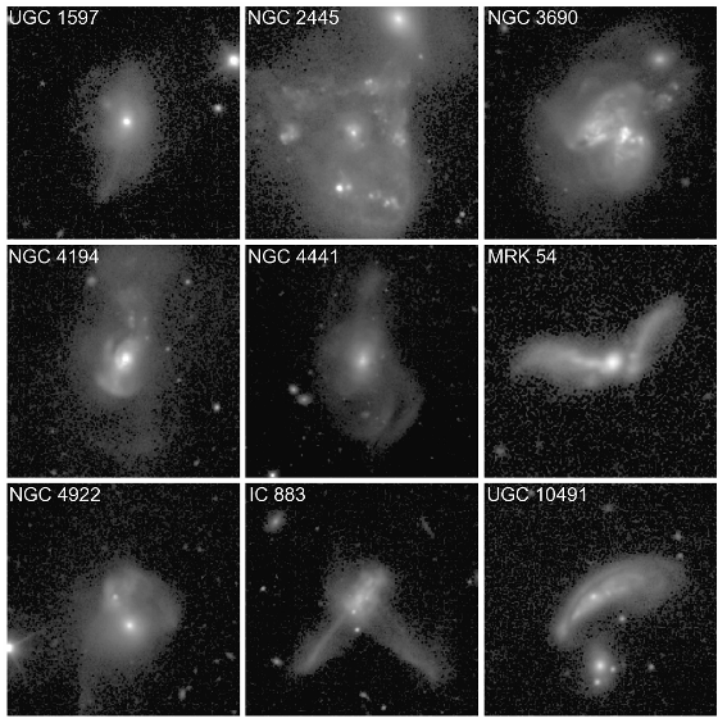

Figure 1.23. *Examples of interacting and merging galaxies*

The types of rings in normal galaxies that define inner, outer and nuclear varieties are likely features that result from internal dynamics (section 1.12). Figure 1.24 shows examples of the extremely rare types of ring-like features that likely result from a cataclysm, such as a galaxy interaction or encounter. Collisional ring galaxies (RGs; upper frames in Figure 1.24) are one type of cataclysmic ring; these are thought to result from a head-on collision between a disk galaxy and a companion (Appleton and

Struck-Marcell 1996). Polar ring galaxies (PRGs; lower frames in Figure 1.24) are a second type; these are thought to originate from the disruption of a small satellite galaxy along a polar orbit around a more massive disk galaxy (Schweizer *et al*. 1983). None of the examples of this type of feature shown in Figure 1.24 are certain cases. The possible PR feature in NGC 2918 is very faint but favorably oriented nearly edge-on (Whitmore *et al*. 1990). The possible case in NGC 4247 may be nearly face-on and less clearcut.

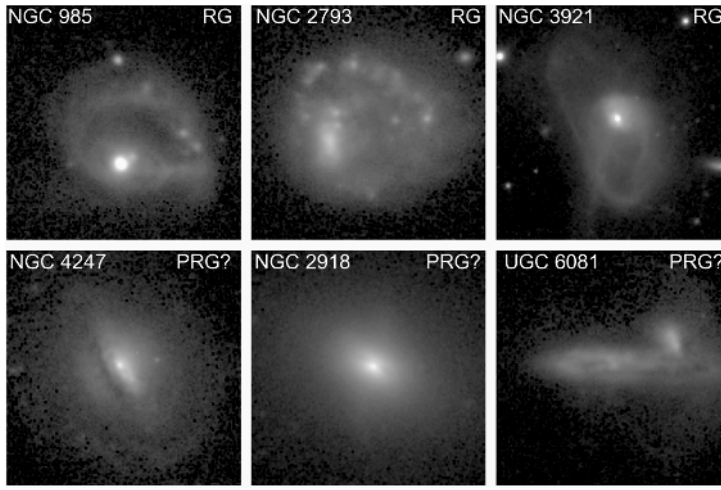

Figure 1.24. *Possible examples of cataclymic ring galaxies. Top row: collisional ring galaxies. Bottom row: polar ring or inclined ring galaxies*

1.10. General properties along the CVRHS sequence

1.10.1. *Morphological systematics*

The classification of a large sample of galaxies in the CVRHS system allows investigation of the systematics of different morphological types and classes, i.e. how aspects of morphology might vary with stage and family. Figure 1.25 first shows the distribution of stages for three galaxy samples: (a) a sample of 1240 galaxies from the Spitzer Survey of Stellar Structure in Galaxies (S^4G; Buta *et al*. 2015); (b) a sample of 441 galaxies from the Analysis of the Interstellar Medium in Isolated Galaxies (AMIGA; Buta *et al*. 2019; Verdes-Montenegro *et al*. 2005); and (c) a sample of 2,628 galaxies from the Extraction of the Forms of Galaxies from Images survey (French acronym: EFIGI; Buta 2019; Baillard *et al*. 2011). Each plot is restricted to galaxies inclined at $\leq 60^\circ$. The three graphs show how the distribution of stages depends sensitively on the selection criteria for a given sample. The S^4G sample is distance-limited and used 21 cm radial velocities to judge distances; this

accounts for the significant emphasis of this sample on extreme late-type (Sd-Sm) spirals and Magellanic irregulars (Im). The EFIGI sample was selected largely on the basis of angular diameter and emphasizes mainly Sb-Sc spirals. The AMIGA sample of isolated spirals is similar in showing an emphasis on Sb-Sc spirals.

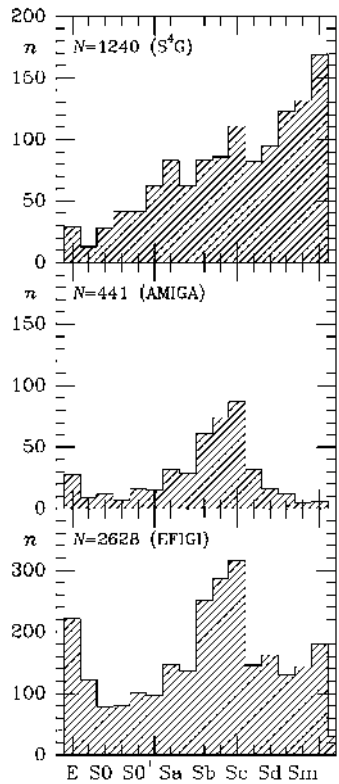

Figure 1.25. *Distribution of CVRHS stages from (a) Buta (2019; EFIGI), (b) Buta et al. (2019; AMIGA) and (c) Buta et al. (2015; S*^{4}*G). The histograms are each restricted to relatively face-on galaxies (*$i \leq 60^\circ$*)*

Figure 1.26 shows the bar, inner variety and outer variety fractions (f_{bar}, f_{IV}, and f_{OV}, respectively) as a function of stage for subsets of EFIGI galaxies inclined $\leq$66°. The numbers are N = (a) 2,440, (b) 749, (c) 1,309, (d) 260 and (e) 2,642 galaxies. Figure 1.26(a) shows that the bar fraction has a minimum near stage Sc, with the highest bar fractions for extreme late-type spirals; Figure 1.26(b) shows that inner rings and well-defined inner pseudorings have the highest fraction around stage Sab; Figure 1.26(c) shows that (s) variety is uncommon for types Sab and earlier, but jumps to $\geq$80% for stages Sc and later; Figure 1.26(d) shows that lenses, ring-lenses and pseudoring-lenses are found mainly among stages Sb and earlier; and Figure 1.26(e)

shows that outer features (rings, pseudorings, lenses and ring lenses) are most common between stages $S0^+$ and Sb. Although outer features are rare for types later than Sb, Figure 1.26 shows a secondary peak among extreme late-type spirals.

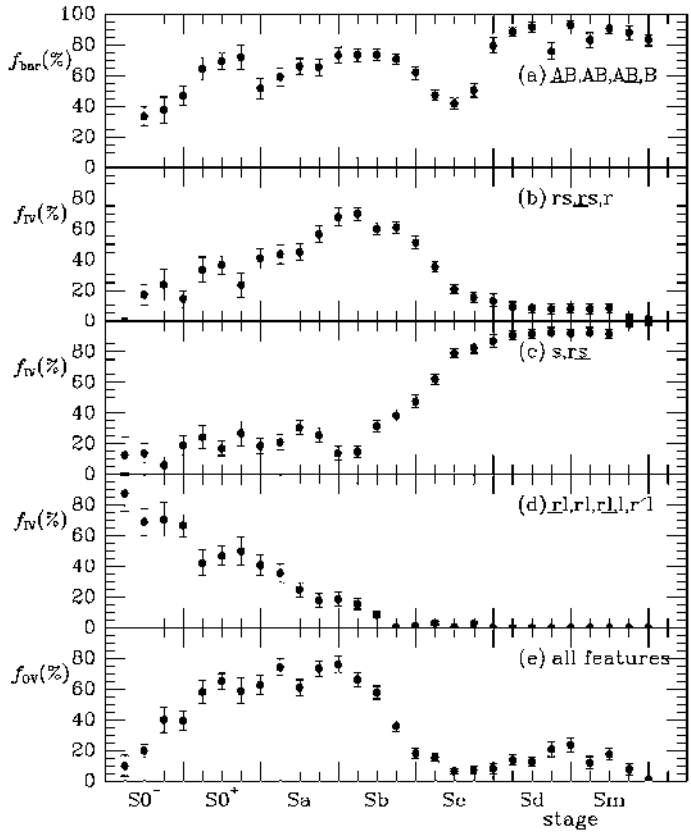

Figure 1.26. *Systematics of CVRHS classifications from Buta (2019; EFIGI). The samples used for these graphs were restricted to inclinations* $\leq 66^\circ$

1.10.2. *Astrophysical systematics*

The CVRHS sequence of galaxy types from ellipticals to irregulars has astrophysical significance. This is because some measured properties of galaxies correlate with position along the sequence. For example, the integrated color index, $(B-V)^o_T$, ranges from $\approx$0.9 for E galaxies to $\approx$0.4 for magellanic irregular galaxies. Over the same range, the color index $(U-B)^o_T$ varies from $\approx$0.5 to -0.2. Color images of galaxies of different types available through the Sloan Digital Sky Survey

show these differences directly. Types earlier than Sa tend to be yellowish, indicating the predominance of an old stellar population, while types Sc and later tend to be mostly bluish, indicating the predominance of a younger stellar population. Intermediate types (Sa to Sbc) show the presence of both populations, with bars and bulges usually yellowish and spiral arms generally bluish. As shown by Buta *et al.* (1994), the color indices of galaxies have a dependence on type that is well approximated by an integral Gaussian, showing little variation from type E to type $S0^+$, followed by a more rapid variation from type S0/a to types Sd and Sdm. This strong dependence on type, which carries into other colors such as $(V-R)_T^o$, $(R-I)_T^o$ and $(B-H)_T^o$ (Buta and Williams 1995; Buta 1995a), has been interpreted in terms of a star formation history where the star formation rate declines exponentially with different decay rates (e.g. Kennicutt *et al*. 1994; Gusev *et al*. 2015).

Other galactic properties that vary along the VRHS sequence include the average surface brightness and HI mass-to-blue luminosity ratio. The average surface brightness ranges from $\approx$12.4 mag arcmin^{-2} for stages E to $S0^+$ to 14.9 mag arcmin^{-2} for stage Im, a factor of 10 drop (Buta *et al*. 1994). This correlation is directly related to one of Hubble's classification criteria for spirals: that Sa galaxies have more prominent central concentrations than do Sc galaxies. The latest stages (Sd-Im) have virtually no central concentration and the lowest average surface brightnesses. Similarly, there is a relatively smooth variation in HI mass-to-blue light ratio across the spiral sequence, ranging from 0.08 at stage S0/a to 0.5 at stage Im, a factor of 6.5 change (Buta *et al*. 1994).

1.11. Other approaches to galaxy classification

The CVRHS system is only one approach to galaxy classification, but it has several advantages: (1) a high focus on features that are likely intimately connected to dynamics and evolution, such as bars, rings and spirals; (2) correlation with star formation history; and (3) the broadest perspective on galaxy morphology without being too unwieldy. However, in the era of large imaging surveys like the Sloan Digital Sky Survey (SDSS; Gunn *et al*. 1998, 2006; York *et al*. 2000), the number of classifiable images of galaxies available is literally in the millions. CVRHS classification by a single individual (for example, Buta 2019) will likely be impractical for samples much larger than 20,000 objects. Another approach to galaxy classification is needed.

Nair and Abraham (2010) provide classifications for 14,034 SDSS galaxies in the redshift range $0.01 < z < 0.1$ in a system similar to the CVRHS. In this case, a single professional astronomer classified each galaxy twice to check for consistency. In the studies of Fukugita *et al*. (2007), Baillard *et al*. (2011) and Ann *et al*. (2015), 3–10 professional astronomers classified either the whole or part of samples of 2253, 4458 and 5836 SDSS galaxies, respectively. In each case, the final classification is an

average of the multiple astronomers, usually after intercomparing results and taking into account "personal equations" of each classifier. One of the largest applications of the multiclassifier approach was made by Kartaltepe *et al*. (2016), who had the input of 65 professional astronomers.

In spite of these efforts, the number of galaxies that have been classified by experts is still relatively small. This led some professional astronomers to try "crowd-sourcing" galaxy classification by engaging with the general public and enlisting the help of "citizen scientists". The first major crowd-sourcing effort is described by Lintott *et al*. (2008) and is called "Galaxy Zoo 1" (GZ1). In GZ1, a web interface was created to display SDSS color images of several hundreds of thousands of galaxies accompanied by a set of "buttons" for selecting rudimentary elements of morphology, such as whether a galaxy is disk-shaped or not. This was followed by "Galaxy Zoo 2" (Willett *et al*. 2013), which allowed classifiers to specify more detail, such as bars, rings and spiral arm character. The classifications in GZ2 were combined using a vote scheme, and an attempt was made to correct the classifications for biases due to resolution and distance. GZ2 provided classifications for nearly 300,000 SDSS galaxies based on about 80,000 participants. Willett *et al*. (2013) provide short abbreviations of these classifications that are compared with the CVRHS classifications of Buta (2019) and Buta *et al*. (2019) in Table 1.12. In these abbreviations, E galaxies are smooth while S galaxies are disk shaped with structure. The other codes are described in Appendix A of Willett *et al*. (2013). Four of the galaxies in Table 1.12 are shown in Figure 1.27.

1.12. Interpretations of morphology

We have seen that galaxy morphology includes a bewildering array of complex structures, and that the evolutionary path that any galaxy took to reach its current morphological state is not obvious. Nevertheless, some reasonable judgments can be made. This section summarizes some aspects of morphology that are well understood, and others that are still largely uncertain.

Galaxy formation: The best current theory of galaxy formation is the Λ Cold Dark Matter model (White and Rees 1978). In this model, galaxy clusters begin as tiny fluctuations in the temperature of the cosmic microwave background radiation that are expanded during the inflationary period to much larger sizes. The fluctuations become "seeds" of cold dark matter within which baryonic matter collects. The formation of collapsing proto-galactic clouds is enhanced by the extra gravity of the dark matter. Whether a galaxy becomes a disk galaxy or a non-disk galaxy depends on how much angular momentum the collapsing cloud has from tidally induced torques due to neighboring clouds (Ryden 1988) and on how effectively it converts its baryonic material into stars. If this conversion is largely complete within a billion or so years after collapse, then the object could become an elliptical galaxy. If instead

the rate of conversion is slower, the proto-galactic cloud may have time to form a disk. Multiple mergers of small objects with this disk-shaped object could lead to the build up of what is generally known as a "classical bulge". This formation scenario is not expected to form a bulge-less, pure disk galaxy, and it is also well-established that some ellipticals have likely formed from mergers of disk-shaped galaxies (Schweizer 1982).

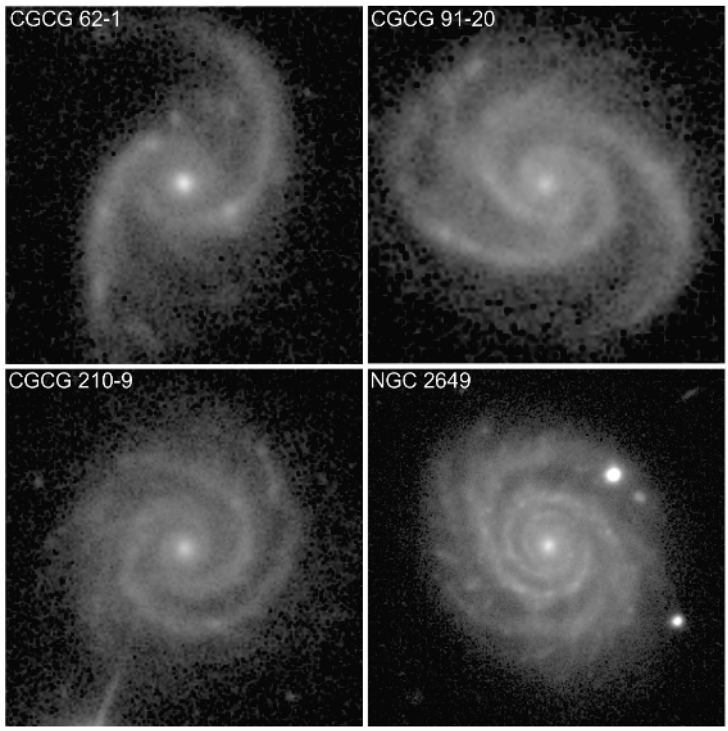

Figure 1.27. *Images of four relatively isolated grand-design spirals (Buta et al. 2019)*

Although the "formative" phase of a galaxy never really ends (i.e. a galaxy may continue to accrete material long after the formation period largely ended, just as planets still accrete interplanetary debris even now), at some point the accretion rate slows down and galactic changes occur very much more slowly. This is the time when *secular evolution* takes over as the dominant mechanism of change (Kormendy and Kennicutt 2004). Secular evolution can be driven entirely by internal processes or by external processes. The idea is that the formative phase of galaxy evolution is fairly rapid compared to secular evolution. To interpret the morphology of some nearby galaxies, we should appeal to secular evolutionary processes.

The origin of S0 galaxies: Dressler (1980) describes the morphology–density relation in rich galaxy clusters, where the most common types of galaxies found are E and S0. This relation, which was first described by Hubble and Humason (1935), led to the general idea, originally proposed by Spitzer and Baade (1951), and elaborated upon by van den Bergh (1976), that S0 galaxies are former spirals that have been stripped of their interstellar gas and dust. The stripping shut down ("quenched") star formation and essentially "killed" the spiral arms. In this scenario, as already noted in section 1.5, S0s cannot be transition stages between ellipticals and spirals, but must form a sequence of decreasing bulge to total luminosity ratio parallel to spirals. This idea is strongly supported by kinematic studies of early-type galaxies (Cappellari *et al*. 2011), photometric studies of dE and dS0 galaxies (Kormendy and Bender 2012) and by multicomponent analysis of a large sample of S0s (Laurikainen *et al*. 2011).

Galaxy	CVRHS type	Willett *et al*. 2013 Type
1	2	3
NGC 5057	(RL)SA(l)0$^+$	E(r)r
NGC 6116	SA(s)a	Sb2m
UGC 10258	(R′)SA(s)ab	Sb2t
NGC 2649	SA(rs)bc	Sc2t
CGCG 62-1	SA(rs)bc	Sc2l
CGCG 91-20	SA(s)bc	Sc2t
CGCG 210-9	SA(s)bc	Sc2t
UGC 4549	SA(rs)cd	Sc?t
IC 2604	SA(s)d	Sc3m
iUGC 9243	SA(s)dm	Sc?m
NGC 4260	SB$_x$(rs)a	SBc2t
NGC 5610	(R′)SB(s)ab	SBc2m
UGC 6854	SB(s)c pec	SBc2m(i)
NGC 5964	SB(s)cd	SBc2m
NGC 5112	SB(s)d	SBc?m
UGC 9215	SB(s)dm	Sd?l(i)

Table 1.1. *Comparison of classifications*

Recent studies of S0 bulges (e.g. Laurikainen *et al*. 2013; Gao *et al*. 2018) have shown that while pseudobulges are present in the class, most S0 bulges are classical in nature. As noted by Gao *et al*. (2018), this strongly rules out any connection between S0s and later-type spiral galaxies (whose bulges are often pseudobulges).

The VRHS actually anticipates a strong relation between S0s and spirals. This is because in the VRHS, inner and outer varieties are carried across the spiral sequence into the S0 domain. The S0 stage sequence, S0$^-$, S0° and S0$^+$, is not the same as the

spiral sequence, but is based on the appearance of decaying patterns, often in the form of rings and lenses, and sometimes as extremely subtle spiral patterns. This suggests a link between S0s and some galaxies that once were spirals. The main problem is that the S0 stage sequence and the spiral stage sequence are not compatible and cannot be considered "parallel".

The sophistication of modern numerical simulations has led to an alternative idea for the origin of some S0s. Rather than simply being stripped spirals, many could be the result of mergers of spirals. This is shown by Eliche-Moral *et al*. (2018), who compare detailed images of S0 galaxies with the results of the GalMer *n*-body merger simulations (Chilingarian *et al*. 2010). Eliche-Moral *et al*. (2018) argue that GalMer major mergers show features that are commonly seen in S0 galaxies, such as ovals and lenses, and also predict a very low bar fraction for S0s. That S0s do indeed have fewer strong bars than spirals was shown by Buta *et al*. (2010) based on the relative bar torque parameter Q_g.

The origin of spiral structure: The most popular idea, known as "density wave" theory, views spiral structure as a rotating pattern through which a galaxy's stars and interstellar gas clouds must pass (Lin and Shu 1964; Toomre 1977; for a more recent review, see Dobbs and Baba 2014). The arms are not material objects, always made of the same stars, but are waves of density where stars and gas clouds experience a temporary "slowdown". It is thought that gas compression in the arms could lead to the enhanced star formation often seen in spiral arms.

Spiral patterns can be leading or trailing in their sense of winding. A leading spiral opens into the direction of rotation, while a trailing spiral opens opposite the direction of rotation. Studies of extinction in tilted spirals shows that trailing arms are the rule (e.g. de Vaucouleurs 1958); leading spirals are very rare but do exist (e.g. Buta *et al*. 2004). A mechanism in density wave theory known as "swing amplification" was identified by Toomre (1981) as a possible way of explaining the long-lived nature of some spirals. The idea uses a combination of differential rotation, epicyclic theory and self-gravity to "swing" a weak leading spiral instability into a much stronger trailing spiral, and explains the preponderance of trailing spiral patterns.

Although density wave theory could account for the velocity perturbations across spiral arms (e.g. Visser 1980), and also could be used to determine spiral pattern speeds (Roberts *et al*. 1975), the theory left open the question of the origin of spiral structure and the impact of a spiral on the evolution of a galaxy. Attention turned to a search for driving mechanisms, which led to a focus on bars and companions. Bars especially became primary features for affecting the secular evolution of galaxies, because a bar can drive gas into the center of a galaxy and build up what is known as a "pseudobulge", or bulge made of disk material. Based on passive orbit studies, it was concluded that secular evolution primarily affects the interstellar gas

distribution, and likely can only change a galaxy of intermediate type by at most one Hubble stage interval (e.g. stage Sbc to Sb) during a Hubble time.

Kormendy (1979) and Kormendy and Norman (1979) brought attention to the role of bars in driving galactic secular evolution. Kormendy and Norman (1979) identified bars as the likely driving mechanism for what they referred to as "global" spiral patterns, i.e. well-defined spirals that extend across an entire galactic disk. If not a bar, then the perturbing effects of a close companion may also drive a density wave spiral. However, there are relatively isolated non-barred galaxies with strong global spiral patterns; Figure 1.27 shows four examples from Buta *et al*. (2019).

Although global spirals are the best-known patterns in galaxies, many galaxies show spiral structure that cannot be called "global". This is because their patterns are mainly in the form of disconnected pieces or ill-defined spirals, called flocculent (Elmegreen 1981). Such spirals have been interpreted in terms of star-forming complexes sheared by differential rotation into short spiral arcs (Gerola and Seiden 1978). Dobbs *et al*. (2018) compare numerical simulations with the ill-defined arms of M33, and conclude that the arms form as a result of gravitational instabilities in the stellar and gaseous distributions, coupled with a high amount of stellar feedback.

Dobbs and Baba (2014) summarize the general view of spiral structure today: "With the possible exception of barred galaxies, spiral arms are transient, recurrent, and initiated by swing-amplified instabilities in the disk".

The origin of bars in spiral galaxies: The general idea has been that bars form through a natural process known as the "bar instability". This is the tendency for an initially axisymmetric but cold stellar disk to naturally form a bar (Hohl 1971). Numerical simulations showed that bars develop in systems where the bulk of the kinetic energy is in the form of ordered motions, i.e. in a rotating disk-shaped galaxy (e.g. Miller and Smith 1979).

Gadotti (2004) argues that while this mechanism seems likely for spirals, it may not be the origin of bars in S0 galaxies because these tend to be found in a cluster environment and have a higher relative abundance of classical bulges (as opposed to pseudobulges). The light-deficient regions around some bars suggest a mechanism where a bar forms at the expense of the disk (Gadotti and de Souza 2003a; Kim *et al*. 2016).

The origin of galactic rings: The general view is that the vast majority of galaxy rings are associated with orbital resonances in galactic disks. A resonance ring is a feature that can, on the basis of morphology and other characteristics, such as star formation, be linked to a specific orbital resonance with a bar, oval or spiral density wave. The idea of a resonance ring first appeared in discussions of density wave theory (for example, Lin 1970), but it was the modeling of barred galaxies that led to a better understanding of these features (Schwarz 1981, 1984).

Resonances occur where $m(\Omega - \Omega_p) = n\kappa$, where Ω is the circular angular velocity, Ω_p is the pattern speed (uniform angular rotation rate of the spiral pattern), κ is the radial (epicyclic) frequency, and m/n is the number of radial oscillations per single orbit in the reference frame rotating at Ω_p. Both Ω and κ are functions of galactocentric radius. The main ring-forming resonances are the outer and inner Lindblad resonances (OLR and ILR, respectively), for which $m = 2$ $n = \pm 1$, and the outer and inner 4:1 resonances (O4R and I4R, respectively), for which $m = 4$ and $n = \pm 1$. In any normal galaxy, there will likely be two ILRs, with the innermost one called the inner ILR (or IILR) and the outermost one called the outer ILR (or OILR). Another important (but not necessarily ring-forming) resonance is the corotation resonance (CR), where $\Omega_p = \Omega$. The locations of all of these resonances can be determined by plotting the curves Ω and $\Omega \pm \kappa/m$ versus galactocentric radius and reading the radii where these functions equal Ω_p.

Support for the resonance idea comes principally from (a) the morphology of galactic rings (Buta and Crocker 1991; Buta 1995b); (2) statistical studies of intrinsic shapes and orientations of galactic rings with respect to bars (Buta 1995b; Comerón *et al*. 2014); and (3) detailed studies and numerical modeling of individual cases such as NGC 3081 (Buta and Purcell 1998) and NGC 6782 (Lin *et al*. 2008). Rings are relatively narrow features, most frequently associated with gas. In particular, nuclear rings are often conspicuous sites of star formation. In general, rings form when gas is accumulating in the bar resonance locations, since the gravity torques from the bar are then canceling out. The angular momentum transport is discussed in detail in Buta and Combes (1996).

Figure 1.28 shows three galaxies from the Catalogue of Southern Ringed Galaxies (Buta 1995b) having well-defined outer resonant features. The white circles in the images show the estimated location of the CR in each galaxy based on the "gap method", a way of determining the radius of the CR using dark gaps lying along the line perpendicular to the bar axis (Buta 2017b). By using this method, and assuming the rotation curves for the galaxies are approximately flat, the schematics show the locations of the other major resonances, I4R, O4R and OLR. The results from these galaxies and 47 others examined by Buta (2017b) provide a consistent picture of systems where R'_2 rings lie slightly outside the OLR, R_1 and R'_1 rings lie near but inside the OLR, and inner rings and bars lie close to the I4R. The ILR was once thought to play a major role in nuclear ring formation, but this view was challenged by Regan and Teuben (2004), who argued that the most reliable interpretation of these features is in terms of an orbit transition region inside the bar.

Ringed galaxies and invariant manifolds: Romero-Gomez *et al*. (2006) proposed an alternative to the resonance interpretation of galactic rings. In this idea, the R_1, R'_1, R'_2 and $R_1R'_2$ subclasses of outer rings and pseudorings in barred galaxies can all be interpreted in terms of invariant manifolds that emanate from the unstable L_1 and L_2 Lagrangian points near the ends of a bar. In this interpretation, rings are not

necessarily resonant features, but are features mapped by the manifolds as tube-guided homoclinic, heteroclinic and escaping chaotic orbits. In homoclinic orbits, a spiral emanates from L_1 or L_2 and closes at L_2 or L_1, respectively, after winding 180°; this is a morphology consistent with R_1 and R_1' rings. In heteroclinic orbits, a spiral emanates from L_1 or L_2 and closes at L_1 or L_2, respectively, after winding 360°; this is a morphology consistent with the double outer ring/pseudoring morphology R_1R_2'. Finally, in an escaping orbit, a spiral emanates from L_1 or L_2 and winds outward, never to intersect the opposing Lagrangian point; these can account for the morphology of R_2' outer pseudorings.

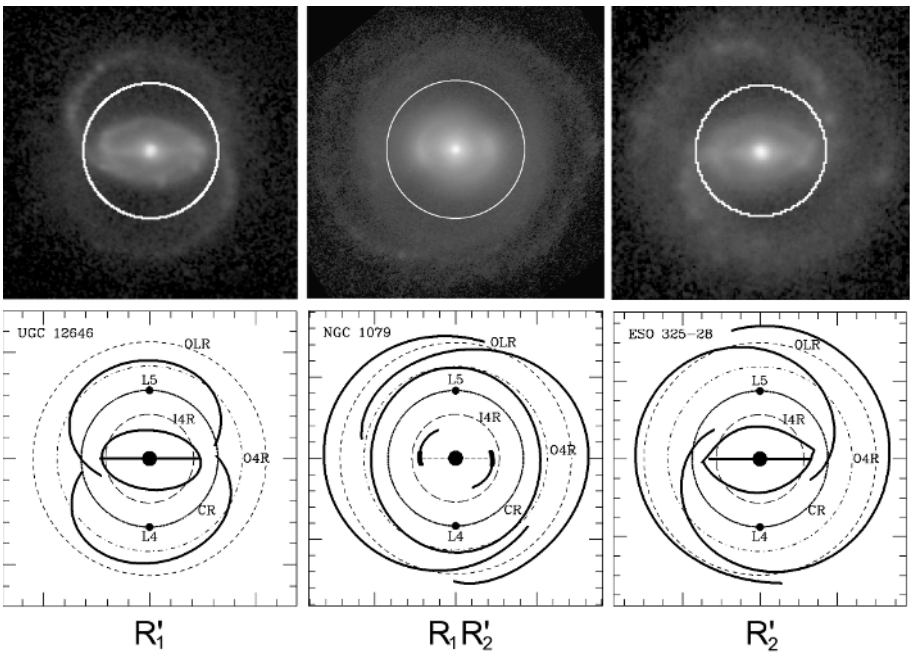

Figure 1.28. *Three galaxies showing outer resonant subclass features. The white circle in each image is the estimated location of the corotation resonance (CR) based on the gap method of Buta (2017b). The schematics show the locations of other resonances relative to visually mapped ring and pseudoring features, assuming a flat rotation curve. The method assumes that light deficits on the line perpendicular to the bar axis trace the location of unstable Lagrangian points L_4 and L_5 (indicated as L4 and L5 each plot). These points are assumed to trace the location of the CR. The other resonances highlighted are the inner 4:1 resonance (I4R), the outer 4:1 resonance (O4R) and the outer Lindblad resonance (OLR)*

The potential-density phase shift and galactic secular evolution: Models of barred galaxies like those of Schwarz (1981, 1984) and Rautiainen and Salo (2000) suggest

that rings are products of the evolution of spiral patterns near resonances. That is, a ring begins as a pseudoring and then evolves into a more closed feature. However, very few galaxies show the influence of resonances as strongly as do cases like NGC 3081 or any galaxy showing outer resonant subclass features. This is because the typical inner variety for spirals is (s), the typical nuclear variety is no nuclear feature and the typical outer variety is no outer feature. The question to ask, then, is not why some galaxies have rings, but why so many do not.

The theoretical work of Zhang (2018 and references therein) challenges previous views on galaxy dynamics and provides a real mechanism for the secular evolution of the stellar distribution of a spiral galaxy, not just the interstellar gas distribution. The galaxy-disk mass distribution, contributed mostly by stellar mass, is part of the so-called "basic state" used to calculate spiral density wave perturbations. In addition to the axisymmetric (i.e. azimuthally averaged) mass distribution, determined observationally from disk surface brightness and color, the basic state specification includes also the axisymmetric rotation speed (with contributions from the halo and bulge, in addition to the contribution from the disk) and velocity dispersion, with all three usually specified as a function of galactocentric radius. The key factor for the evolution of the basic-state mass distribution is an azimuthal phase shift (phase offset in angles) between a self-consistent spiral perturbation potential, and the density this potential gives rise to. The spiral can arise as a mode in an initially featureless disk, and if it can achieve a quasi-steady state, angular momentum can be taken away from the inner disk, transferred outward and deposited onto the outer disk, leading to the slow buildup of a central mass concentration and an extended outer disk.

The main departure of Zhang's work from previous studies of galactic dynamics is the elevated role of collective effects on the dynamical evolution of galaxies. This refers to the correlated small-angle scatterings stars would experience as they move across the spiral density wave crest. The density wave itself was shown in Zhang's work to be collisionless shocks related to "dissipative structures". Another important aspect of the work is that the phase shift is not simply an abstract concept from potential theory, but is manifestly measurable from any image which approximates the stellar mass distribution. From such images, one can derive a graph of the phase shift as a function of radius, and in such a graph a single mode appears as a single positive bump followed by a single negative bump (e.g. Buta and Zhang 2009). The point where the phase shift changes from positive to negative is the location of the mode's CR, which is generally considered the most important resonance for any model pattern in a galaxy. This location is also the divide between radial mass inflow and outflow patterns.

1.13. Artificial galaxies and the future of galaxy classification

Galaxy classification will continue to have value in extragalactic studies for several reasons: (1) the continuing availability and also planned production of

high-quality, multifilter, ground-based and space-based, digital imaging surveys; (2) the usefulness of the Internet for "crowd sourcing" galaxy classification through the Galaxy Zoo project and its offshoots; (3) the sophistication of modern numerical simulation programs that can make model galaxies that are so realistic that they can be classified like real galaxies; and (4) the advances in artificial neural networks that have made automatic galaxy classification feasible on a scale not previously achieved.

The SDSS will continue to play a role in all of this through its many data releases, the latest of which, DR 16, will occur in December 2019. In general, SDSS images are of very high quality for both qualitative and quantitative studies of galaxies. However, the SDSS footprint has largely excluded the southern sky. The Panoramic Survey Telescope and Rapid Response System (Pann-STARRS; Kaiser *et al*. 2010) cover the part of the sky north of declination $-30°$. Although many of the Pan-STARRS images have peculiar defects, many are still very useful. Sophisticated databases in progress, or planned, include the Dark Energy Camera Legacy Survey (DECaLS; Blum *et al*. 2016), the Kilo-Degree Survey (KiDS; de Jong *et al*. 2013), the Hyper Suprime-Cam Subaru Strategy Program (HSC-SSP; Aihara *et al*. 2018), the Large Synoptic Survey Telescope (LSST; Ivezič *et al*. 2019), the European Space Agency Euclid mission (Laureijs *et al*. 2012) and the Wide Field Infrared Survey Telescope (WFIRST; Gehrels *et al*. 2015). Although the goals of many of these new surveys are mainly cosmology related (with focus on dark energy and dark matter), the public availability of these imaging databases will facilitate deeper, higher resolution studies of both nearby and very distant galaxies.

The Illustris project (Vogelsberger *et al*. 2014) is one of the most comprehensive simulational surveys of galaxies ever made. The project takes advantage of advances in simulation programming, storage space and computing power, and includes as many physical processes as relevant, such as feedback due to AGN, supernovae, and supermassive black holes, mass and internal dynamics of dark and baryonic matter and the efficacies of star formation, to produce synthetic galaxies at such a realistic level that, once converted into observational units, can match the morphology of many SDSS galaxies. An expert morphologist would be able to examine these artificial galaxies and classify many within the Hubble tuning fork or in some other manner. Snyder *et al*. (2015) show using non-parametric measures of galaxy morphology that Illustris synthetic galaxies approximate $z \approx 0$ galaxies well enough to match the correlation between star formation and galaxy morphology. A great advantage of the project is the ability of the survey to show how different synthetic galaxies evolve under the conditions of the models. For example, followed to high redshifts, the Illustris models reproduce the observed characteristic that galaxies become more irregular at higher redshifts than at lower redshifts (Genel *et al*. 2014).

Like the SDSS, many of the new digital imaging surveys will provide detailed information on the morphologies of literally *millions of galaxies* over a wide range

of redshift. The classifications of these galaxies are critical to cosmological studies of galaxy formation and evolution. While significant subsets of galaxies are and will continue to be classified visually by single or multiple experts, the vast majority of galaxies will have to be classified in other ways. The Galaxy Zoo project (Lintott *et al*. 2008) recognized that there will never be enough professional experts to classify hundreds of thousands of galaxies, and instead enlisted the volunteer assistance of tens of thousands of non-expert "citizen scientists" to classify galaxies in enough detail to be cosmologically useful. The Galaxy Zoo Team did not require that volunteers use the CVRHS system to classify galaxies, but instead allowed volunteers to select a few basic characteristics through the use of a small number of buttons in a web interface. How GZ2 classifications compare with some CVRHS classifications was shown in section 1.11. However, as effective as Galaxy Zoo has been for large-scale galaxy classification, there will still be hundreds of thousands or millions of galaxies that will need to be classified.

Dieleman *et al*. (2015) describe an effective method for automatic classification that uses deep learning with convolutional neural networks. The method inputs multifilter SDSS images of a large sample of galaxies having known morphological classifications. Domínguez Sánchez *et al*. (2019) use the crowd-sourced GZ2 classifications and the T-classifications of Nair and Abraham (2010) to obtain automatic classifications of 670,000 galaxies.

Many other aspects of galaxy morphology are worth examining; these are described in more detail in the review articles by Buta (2012, 2013).

1.14. References

Abbott, C.G., Valluri, M., Shen, J., *et al*. (2017). *MNRAS*, 470, 1526.

Aihara, H., *et al*. (2018). *PASJ*, 70, 84.

Ann, H.B., Seo, M., Ha, D.K. (2015). *ApJS*, 217, 27.

Appleton, P., Struck-Marcell, C. (1996). *FCPh*, 16, 111.

Athanassoula, E. (2016) In *Galactic Bulges,* Laurikainen, E., Peletier, R., Gadotti, D. (eds). ASSL, vol. 418. Springer International Publishing, Switzerland, p. 391.

Athanassoula, E., Rodonov, S.A., Peschke, N., *et al*. (2016). *ApJ*, 821, 90.

Baillard, A., Bertin, E., de Lapparent, V., *et al*. (2011). *A&A*, 532, 74.

Bertola, F., Galletta, G. (1978). *ApJ*, 226, L115.

Blum, R.D., *et al*. (2016). *BAAS*, 228, 317.

Bournaud, F., Combes, F. (2002). *A & A*, 392, 83.

Buta, R. (1995a). *ApLC*, 31, 109.

Buta, R. (1995b). *ApJS*, 96, 39.

Buta, R. (2012). Galaxy morphology. In *Secular Evolution of Galaxies*, Falcón-Barroso, J., Knapen, J.H. (eds). Cambridge University Press, Cambridge, 155.

Buta, R. (2013). Galaxy morphology. In *Planets, Stars, & Stellar Systems, Vol. 6*, Oswalt, T.D., Keel, W. C. (eds). Springer, Dordrecht, p. 1.

Buta, R. (2019). *MNRAS*, 488, 590.

Buta, R.,Verdes-Montenegro, L., Damas-Segovia, A., *et al*. (2019). *MNRAS*, 488, 2175.

Buta, R., Block, D.L. (2001). *ApJ*, 550, 243.

Buta, R., Combes, F. (1996). *FCPh*, 17, 95.

Buta, R., Crocker, D.A. (1991). *AJ*, 102, 1715.

Buta, R., Purcell, G.B. (1998). *AJ*, 115, 484.

Buta R., Williams K.L. (1995). *AJ*, 109, 543.

Buta, R., Zhang, X. (2009). *ApJS*, 182, 559.

Buta, R., Byrd, G.G., Freeman, T. (2004). *AJ*, 127, 1982.

Buta, R., Corwin, H.G., Odewahn, S.C. (2007). *The de Vaucouleurs Atlas of Galaxies*. Cambridge University Press, Cambridge.

Buta, R., Laurikainen, E., Salo, H., *et al*. (2010). *ApJ*, 721, 259.

Buta, R., Mitra, S., de Vaucouleurs, G., *et al*. (1994). *AJ*, 107, 118.

Buta, R., *et al*. (2015). *ApJS*, 217, 32.

Byrd, G.G., Rautiainen, P., Salo, H., *et al*. (1994). *AJ*, 108, 476.

Capaccioli, M. (1987). In *The Structure and Dynamics of Elliptical Galaxies*, de Zeeuw, T. (ed.). *IAU Symposium* 127, Reidel, Dordrecht, p. 47.

Cappellari, M., *et al*. (2011). *MNRAS*, 416, 1680.

Chilingarian, I.V., Di Matteo, P., Combes, F., *et al*. (2010). *A&A*, 518, A61.

Combes, F., Sanders, R.H. (1981). *A&A*, 96, 164.

Comerón, S., Knapen, J.H., Beckman, J.E., *et al*. (2010). *MNRAS*, 402, 2462.

Comerón, S., *et al*. (2014). *A&A*, 562, 121.

Crocker, D.A., Baugus, P.D., Buta, R. (1996). *ApJS*, 105, 353.

Curtis, H.D. (1918). *Publ. Lick Obs.*, 13, 9.

de Jong, J.T.A., *et al*. (2013). *The Messenger*, 154, 44.

de Lapparent, V., Baillard, A., Bertin, E. (2011). *A&A*, 532, 74.

de Vaucouleurs, G. (1948). *Annales d'Astrophysique*, 11, 247.

de Vaucouleurs, G. (1958). *ApJ*, 127, 487.

de Vaucouleurs, G. (1959). *Handbuch der Physik*, 53, 275.

de Vaucouleurs, G. (1963). *ApJS*, 8, 31.

de Vaucouleurs, G., Freeman, K.C. (1972). *Vistas in Astronomy*, 14, 163.

de Vaucouleurs, G., de Vaucouleurs, A., Corwin, H.G., *et al*. (1991). *Third Reference Catalogue of Bright Galaxies*. Springer, New York.

Dieleman, S., Willett, K.W., Dambre, J. (2015). *MNRAS*, 450, 1441.

Dobbs, C., Baba, J. (2014). *PASA*, 31, e035.

Dobbs, C.L., Pettitt, A.R., Corbelli, E., *et al*. (2018). *MNRAS*, 478, 3793.

Domínguez Sánchez, H., Huertas-Company, M., Bernardi, M., *et al*. (2018). *MNRAS*, 476, 3661.

Domínguez Sánchez, H., *et al*. (2019). *MNRAS*, 484, 93.

Dressler, A. (1980). *ApJ*, 236. 351.

Dreyer, J.L.E. (1888). A new general catalogue of nebulae and clusters of stars. *Mem. Roy. Astr. Soc.*, 49, 1.

Eliche-Moral, M.C., Rodríguez-Pérez, C., Borlaff, A., *et al*. (2018). *A&A*, 617, A113.

Elmegreen, D.M. (1981). *ApJS*, 47, 229.

Eskridge, P., *et al*. (2000). *AJ*, 119, 536.

Fasano, G., Bonoli, C. (1989). *A&AS*, 79, 291.

Fukugita, M., *et al*. (2007). *AJ*, 134, 579.

Gadotti, D. (2004). *PASP*, 116, 591.

Gadotti, D., de Souza, R. (2003a). *Ap&SS*, 284, 527.

Gadotti, D., de Souza, R. (2003b). *ApJ*, 583, L75.

Gao, H., Ho, L.C., Barth, A.J., *et al*. (2018). *ApJ*, 867, 100.

Garcia-Gómez, C., Athanassoula, E., Barberà, C., *et al*. (2017). *A&A*, 601, A132.

Gehrels, N., *et al*. (2015). *J. Phys., Conf. Ser.* 610, 012007.

Genel, S. *et al*. (2014). *MNRAS*, 445, 175.

Gerola, H., Seiden, P.E. (1978). *ApJ*, 223, 129.

Graham, A.W. (2013). In *Planets, Stars, and Stellar Systems, Vol. 6*, Oswalt, T.D., Keel, W. C. (eds). Springer, Dordrecht, p. 91.

Grouchy, R.D., Buta, R., Salo, H., *et al*. (2010). *AJ*, 139, 2465.

Gunn, J.E., Carr, M., Rockosi, C., *et al*. (1998). *AJ*, 116, 3040.

Gunn, J.E., *et al*. (2006). *AJ*, 131, 233.

Gusev, A.S., *et al*. (2015). *A&A*, 59, 899.

Hohl, F. (1971). *ApJ*, 168, 343.

Hubble, E. (1926). *ApJ*, 64, 321.

Hubble, E. (1936). *The Realm of the Nebulae*. Yale University, New Haven, CT.

Huang, S., Ho, L.C., Peng, V.Y., *et al*. (2013). *ApJ*, 766, 47.

Hubble, E., Humason, M.L. (1931). *ApJ*, 74, 43.

Ivezi, Z., *et al*. (2019). *ApJ*, 873, 111.

Kaiser, N., *et al*. (2010). In *Proceedings of SPIE*, Vol. 7733, Ground-based and Airborne Telescopes III, 77330E.

Kartaltepe, J.S., *et al*. (2016). *ApJS*, 221, 11.

Keeler, J.E. (1899). *MNRAS*, 60, 128.

Kennicutt, R.C., Tambln, P., Congdon, C.W. (1994). *ApJ*, 435, 22.

Kim, T., Gadotti, D., Athanassoula, E., *et al*. (2016). *MNRAS*, 462, 3430.

Knapen, J., James, P.A. (2009). *ApJ*, 698, 1437.

Koopmann, R., Kenney, J.D.P. (2004). *ApJ*, 613, 866.

Kormendy, J. (1979). *ApJ*, 227, 714.

Kormendy, J., Bender, R. (1996). *ApJ*, 464, 119.

Kormendy, J., Bender, R. (2012). *ApJS*, 198, 2.

Kormendy, J., Djorgovski, S. (1989). *ARAA*, 27, 235.

Kormendy, J., Kennicutt, R. C. (2004). *ARA&A*, 42, 603.

Kormendy, J., Norman, C. (1979). *ApJ*, 233, 539.

Laureijs, R., *et al*. (2012). *SPIE Proceedings,* Space Telescopes and Instrumentation: Optical, Infrared, and Millimeter Wave, 8442, OT.

Laurikainen, E., Salo, H., Athanassoula, E., *et al*. (2013). *MNRAS*, 430, 3489.

Laurikainen, E., Salo, H., Buta, R., *et al*. (2011). *MNRAS*, 418, 1452.

Lin, C.C. (1970). In *The Spiral Structure of Our Galaxy*, Becker, W., Kontopoulos, G.I. (eds). *IAU Symposium 38*, Reidel, Dordrecht, p. 377.

Lin, C.C., Shu, F.H. (1964). *ApJ*, 140, 646.

Lin, L.-H., Yuan, C., Buta, R. (2008). *ApJ*, 684, 1048.

Lintott, C., *et al*. (2008). *MNRAS*, 389, 1179.

Lundmark, K. (1926). *Archive for Mathematics, Astronomy, and Physics*, 19(8), 1.

Lutticke, R., Dettmar, R.-J. (1999). *Ap&SS*, 265, 393.

Martinez-Valpuesta, I., Knapen, J.H., Buta, R. (2007). *AJ*, 134, 1863.

Miller, R. H., Smith, B.F. (1979). *ApJ*, 227, 785.

Morgan, W.W. (1958). *PASP*, 70, 364.

Nair, P., Abraham, R.G. (2010). *ApJ*, 714, L260.

Nieto, J.L. (1988). *Bol. Acad. Nac. Cienc. Cordoba, Argentina*, 58(3-4), 239.

Norman, C.A., Sellwood, J., Hasan, H. (1996). *ApJ*, 462, 114.

Rautiainen, P., Salo, H. (2000). *A&A*, 362, 465.

Regan, M., Teuben, P. (2004). *ApJ*, 600, 595.

Reynolds, J.H. (1920). *MNRAS*, 80, 746.

Roberts, W.W., Roberts, M.S., Shu, F.H. (1975). *ApJ*, 196, 381.

Romero-Gómez, M., Masdemont, J.J., Athanassoula, E., *et al*. (2006). *A&A*, 453, 39.

Ryden, B.S. (1988). *ApJ*, 329, 589.

Sandage, A. (1961). *The Hubble Atlas of Galaxies*, Carnegie Inst. of Wash., Washington, D.C., Publ. no. 618.

Sandage, A., Binggeli, B. (1984). *AJ*, 89, 919.

Schwarz, M.P. (1981). *ApJ*, 247, 77.

Schwarz, M.P. (1984). *MNRAS*, 209, 93.

Schweizer, F. (1982). *ApJ*, 252, 455.

Schweizer, F. (1987). In *The Structure and Dynamics of Elliptical Galaxies*, IAU Symposium 127, de Zeeuw, T. (ed). Reidel, Dordrecht, p. 109.

Schweizer, F., Seitzer, P. (1988). *ApJ*, 328, 88.

Schweizer, F., Whitmore B.C., Rubin V. (1983). *AJ*, 88, 909.

S'ersic, J.L. (1968). *Atlas de Galaxias Australes*. Observatorio Astronomico, Cordoba, Argentina.

Sheth, K., *et al*. (2008). *ApJ*, 675, 1141.

Snyder, G.F., *et al*. (2015). *MNRAS*, 454, 1886.

Spitzer, L., Baade, W. (1951). *ApJ*, 113, 413.

Toomre, A. (1977). *ARA&A*, 15, 437.

Toomre, A. (1981). In *The Structure and Evolution of Normal Galaxies*, Fall, S.M., Lynden-Bell, D. (eds), Cambridge University Press, Cambridge, p. 111

Tsatsi, A., Lyubenova, M., van de Ven, G., *et al*. (2017). *A&A*, 606, A62.

van den Bergh, S. (1976). *ApJ*, 206, 883.

Verdes-Montenegro, L., Sulentic, J., Lisenfeld, U., *et al*. (2005). *A&A*, 436, 443.

Visser, H. (1980). *A&A*, 88, 159.

Vogelsberger, M., *et al*. (2014). *MNRAS*, 444, 1518.

White, S.D.M., Rees, M.J. (1978). *MNRAS*, 183, 341.

Whitmore, B.C., Lucas, R.A., McElroy, D.B., *et al*. (1990). *AJ*, 100, 1489.

Willett, K.W., *et al*. (2013). *MNRAS*, 435, 2835.

Wolf, M. (1908). Publ. of the Astrophysical Institute, Koenigstuhl-Heidelberg, 3, 109.

Yagi, M., Yoshida, M., Komiyama, Y., *et al*. (2010). *AJ*, 140, 1814.

York, D.G., Adelman, J., Anderson, J.E., *et al*. (2000). *AJ*, 120, 1579.

Zhang X. (2018). *Dynamical Evolution of Galaxies*. de Gruyter GmbH, Berlin/Boston.